Assimilating summer sea-ice thickness observations improves Arctic sea-ice forecast

Ruizhe Song[1], Longjiang Mu[2], Svetlana Loza[3], Frank Kauker[4], and Xianyao Chen[1]

[1]Ocean University of China
[2]Laoshan Laboratory
[3]Alfred Wener Institute for Polar and Marine Research
[4]OASys

April 16, 2024

Abstract

Proper Arctic sea-ice forecasting for the melt season is still a major challenge because of the recent lack of reliable pan-Arctic summer sea-ice thickness (SIT) data. A new summer CryoSat-2 SIT observation data set based on an artificial intelligence algorithm may alleviate this situation. We assess the impact of this new data set on the initialization of sea-ice forecasts in the melt seasons of 2015 and 2016 in a coupled sea ice-ocean model with data assimilation. We find that the assimilation of the summer CryoSat-2 SIT observations can reduce the summer ice-edge forecast error. Further, adding SIT observations to an established forecast system with sea-ice concentration assimilation leads to more realistic short-term summer ice-edge forecasts in the Arctic Pacific sector. The long-term Arctic-wide SIT prediction is also improved. In spite of remaining uncertainties, summer CryoSat-2 SIT observations have the potential to improve Arctic sea-ice forecast on multiple time scales.

Assimilating summer sea-ice thickness observations improves Arctic sea-ice forecast

Ruizhe Song[1,2,3,4], Longjiang Mu[2], Svetlana N. Loza[3,5], Frank Kauker[3], Xianyao Chen[1,2]

[1]Frontier Science Center for Deep Ocean Multispheres and Earth System and Physical Oceanography Laboratory, Ocean University of China, Qingdao, China
[2]Laoshan Laboratory, Qingdao, China
[3]Alfred Wegener Institute, Helmholtz Centre for Polar and Marine Research, Bremerhaven, Germany
[4]Academy of the Future Ocean, Ocean University of China, Qingdao, China
[5]Shirshov Institute of Oceanology, Russian Academy of Sciences, Moscow, Russia

Key Points:

- Assimilating summer CryoSat-2 sea-ice thickness (SIT) observations makes more skillful Arctic ice-edge forecasts on multiple time scales.
- The long-term SIT forecasts improve with the assimilation of summer CryoSat-2 SIT observations.
- Further refinement is needed for summer CryoSat-2 SIT observations.

Corresponding author: Longjiang Mu, `ljmu@qnlm.ac`

Abstract

Proper Arctic sea-ice forecasting for the melt season is still a major challenge because of the recent lack of reliable pan-Arctic summer sea-ice thickness (SIT) data. A new summer CryoSat-2 SIT observation data set based on an artificial intelligence algorithm may alleviate this situation. We assess the impact of this new data set on the initialization of sea-ice forecasts in the melt seasons of 2015 and 2016 in a coupled sea ice-ocean model with data assimilation. We find that the assimilation of the summer CryoSat-2 SIT observations can reduce the summer ice-edge forecast error. Further, adding SIT observations to an established forecast system with sea-ice concentration assimilation leads to more realistic short-term summer ice-edge forecasts in the Arctic Pacific sector. The long-term Arctic-wide SIT prediction is also improved. In spite of remaining uncertainties, summer CryoSat-2 SIT observations have the potential to improve Arctic sea-ice forecast on multiple time scales.

Plain Language Summary

Arctic sea ice is rapidly declining due to global warming, especially in summer. Accurate sea-ice forecasting is important to understand the potential influence of these changes and devise effective responses. The performance of sea-ice forecasts highly depends on the accuracy of the initial sea-ice states. So refining the initial conditions of sea-ice forecasts with satellite observations is a common way to reduce forecast errors. However, obtaining reliable summer pan-Arctic satellite sea-ice thickness (SIT) data is challenging due to complex ice-surface conditions in summer. A new artificial-intelligence-based summer SIT satellite data product may mitigate this situation. We integrate this data set into a sea-ice forecast system to evaluate its impact on forecast accuracy. We find that the new summer satellite SIT data can reduce short-term ice-edge location forecast errors and benefit long-term SIT forecasts.

1 Introduction

Arctic sea ice is declining at unprecedented speed (Rothrock et al., 1999; Comiso et al., 2008; Kwok & Rothrock, 2009; Stroeve et al., 2012), which would pose challenges to climatic and ecological stakeholders (Landrum & Holland, 2020). The Arctic Passage, opening up with the gradually melting summer sea ice, calls for accurate Arctic sea-ice prediction from daily to seasonal scales (Jung et al., 2016).

Accurate initialization of sea-ice state is vital for predicting Arctic sea ice (e.g., Blanchard-Wrigglesworth et al., 2011; Guemas et al., 2016; Xie et al., 2016; Dirkson et al., 2017; Bushuk et al., 2022). The assimilation of sea-ice concentration (SIC) has improved the short-term sea-ice forecasts greatly as documented in the literature, and is now widely used at forecasting centers (e.g., Hebert et al., 2015; Lemieux et al., 2015). Sea-ice thickness (SIT) persists longer, therefore assimilation of SIT raises long-term sea-ice forecast skills even stronger (Day, Hawkins, & Tietsche, 2014; Shu et al., 2021; Mu et al., 2022).

However, the potential impacts of summer SIT observations on sea-ice forecasts are not examined comprehensively yet due to a lack of data. An effective retrieval method for the remotely sensed SIT from May to September was missing (Laxon et al., 2013; Ricker et al., 2014). The complex summer ice-surface conditions restrict the application of classical algorithms designed for winter conditions. For instance, melt ponds which occupy a huge fraction of the sea-ice surface in the melt seasons (Maykut et al., 1992) complicate the classification algorithms (Lee et al., 2018; Tilling et al., 2019) and introduce large uncertainties due to increased moisture in the snow (Drinkwater, 1991). On the other hand, in-situ Arctic SIT observations are rather scarce and localized. They can hardly be used in basin-scale assimilation systems.

In a recent study, Dawson et al. (2022) presented the first estimate of pan-Arctic summer sea-ice freeboard from radar altimeter by using a 1D convolutional neural network (CNN) to distinguish ice leads from melt ponds. Landy et al. (2022) converted summer CryoSat-2 radar freeboard to SIT and applied further corrections. The spring predictability barrier of the Arctic sea ice (e.g., Day, Tietsche, & Hawkins, 2014; Bushuk et al., 2017) suggests that sea-ice forecast should benefit from the initialization with SIT in the melt season (Bushuk et al., 2020). Therefore, it presents an opportunity to explore the extent to which the summer SIT observation could improve the real-time forecast skill. Min et al. (2023) demonstrated that assimilation of summer SIT corrects the overestimation in the Combined Model and Satellite Thickness (CMST; Mu et al., 2018b) product. Y.-F. Zhang et al. (2023) found that the assimilation of May to August CryoSat-2 SIT anomalies improves local SIC and sea-ice extent (SIE) forecasts in September. However, the influence of assimilating summer CryoSat-2 SIT observations on short-term sea-ice forecast in summer and on long-term forecast extending beyond September still needs to be investigated further.

In this study, we focus on the impact of summer SIT observations on the daily and seasonal forecast skills of a sea-ice prediction modelling system. In particular, we perform a series of short- and long-term ensemble sea-ice forecasts where the sea ice-ocean initial state is constrained by the summer CryoSat-2 SIT or where these data are not used. The benefits and challenges of using these new SIT data are evaluated and critically discussed using independent sea-ice data.

2 Data and Methods

2.1 The coupled sea ice-ocean model

We use a regional coupled sea ice-ocean model driven by atmospheric forecasts to configure the sea ice-ocean forecast system. The model is based on the Massachusetts Institute of Technology general circulation model (MITgcm; Marshall et al., 1997) and covers the pan-Arctic region with a horizontal resolution of around 18 km as in Losch et al. (2010). The sea-ice model uses a viscous-plastic rheology (Hibler III, 1979; J. Zhang & Hibler III, 1997) and a so called zero-layer thermodynamic formulation without heat capacity (Semtner, 1976; Parkinson & Washington, 1979). The readers are referred to Losch et al. (2010) and Nguyen et al. (2011) for more details on the model.

2.2 Data assimilation and forecast

The summer data assimilation system is initialized from restart files generated by CMST (Mu et al., 2018b) simulation with 11 ensemble members. CMST combines model physics with information from remote-sensed SIT and SIC observations. It successfully reproduces the spatio-temporal sea-ice variations (Mu et al., 2018b). The summer data assimilation and forecast strategy follows Mu et al. (2017) and Mu et al. (2019). A Local Error Subspace Transform Kalman Filter (Nerger et al., 2012) coded within the Parallel Data Assimilation Framework (Nerger et al., 2005) is used to assimilate the summer SIT and SIC observations separately or simultaneously. Then, the summer ensemble forecasts start from the new individual analyses and the model is integrated forced by the atmospheric forecasts (cf. Section 2.3).

The CryoSat-2 summer SIT data set is derived from local variations in the CryoSat-2 radar echo response using a deep learning method (Dawson et al., 2022; Landy et al., 2022). This is the first estimate of pan-Arctic summer SIT from satellite observations. However, the accuracy of the CryoSat-2 summer SIT still needs to be further improved after the correction introduced by Landy et al. (2022), for example over the regions north of the Greenland and the Canadian Arctic Archipelago (CAA). The summer SIT is assimilated into the system on a daily basis using the observations linearly interpolated between two biweekly records. Considering the shortcomings of the summer SIT over thick ice regions, practical experience suggests that the observation uncertainties should be set higher than the original values over thick ice regions, while still using the provided errors over thin ice regions (Supporting Information). The SIC data used in the assimilation are computed at the French Research Institute for Exploitation of the Sea (IFREMER) based on the 85-GHz SSM/I and SSM/IS channels (Kaleschke et al., 2001; Spreen et al., 2008; Kern et al., 2010). The uncertainty of the SIC observation is set to a constant value of 0.25 following Yang, Losa, Losch, Jung, and Nerger (2015) and Yang et al. (2016).

The short-term ensemble assimilation and forecast experiments are driven by the 174-hour atmospheric ensemble forecasts from the United Kingdom Met Office (UKMO) Ensemble Prediction System (EPS; Bowler et al., 2008). For the long-term prediction, the ensemble members are driven by deterministic atmospheric forcing (single member). The hourly European Centre for Medium-Range Weather Forecasts Reanalysis v5 (ERA-5; Hersbach et al., 2020) is used as the atmospheric forcing during the data assimilation, while the atmospheric forecasts from the National Center for Environmental Prediction Climate Forecast System Version 2 (CFSv2; Saha et al., 2014) are used for the 9-month long-term forecasts.

2.3 Experiment design

In order to investigate the potential impact of the CryoSat-2 summer SIT on sea-ice forecasts, this study designs both short-term (7 days) and long-term (270 days) forecasts (Table. 1). These experiments are conducted over different months. The short-term experiments in 2015, which cover the melt season, start from the CMST restart files on May 1, May 31, June 30, July 30, and August 29, respectively. Each forecast experiment lasts for 30 days and on each day a 7-day sea-ice forecast is run using the atmospheric forcing from the daily UKMO ensemble forecasts. No data assimilation is applied in the control run of the short-term forecasts (Short-CTRL). The Short-SIT experiments assimilate only the CryoSat-2 summer SIT data, and the Short-SIC experiments assimilate only the SSMI/SSMIS SIC data, while both data sets are assimilated in the Short-SICSIT experiments. For the 2016 experiments, only the start dates are changed to match the available restart files from CMST (Table. 1).

The long-term forecast experiments are designed to diagnose the persistence of the assimilated CryoSat-2 summer SIT over the months from the melt season to the freezing season. The Long-SIT experiments with SIT assimilation start each summer month from CMST restart files and a daily data assimilation step iterating over 15 days is performed to mitigate abrupt SIT changes. Over that period, ERA5 atmospheric reanalysis forcing is used. Then, the 270-day sea-ice forecasts start from the sea-ice analysis restart files and are forced by the CFSv2 operational atmospheric forecasts. No data assimilation is performed in the Long-CTRL experiments. The forecast start dates are listed in Table 1.

2.4 Verification

Simulation output from the Pan-Arctic Ice-Ocean Modeling and Assimilation System (PIOMAS; J. Zhang & Rothrock, 2003) is employed for the comparison with the assimilation results. PIOMAS is constrained by SIC and sea surface temperature observations. Its modeled SIT has been validated to be comparable to in-situ observations and has been widely used in previous studies.

The integrated ice-edge error (IIEE; Goessling et al., 2016) is used to quantify the skill of the short-term ice-edge forecasts. It measures the discrepancy between the forecasted and observed SIE. The reference observation used in this study is the NOAA/NSIDC Climate Data Record (CDR) of Passive Microwave Sea Ice Concentration Version 4 (Meier et al., 2021).

To validate the skill of the long-term sea-ice forecast, we compute the IIEE and the RMSD of SIT against various other products and in-situ observations. The IIEE is com-

Table 1. Summary of forecast experiments design. Short: short-term forecast. Long: long-term forecast.

Experiment	Assimilated data	Forecast duration (days)	Atmospheric forcing during assimilation	Atmospheric forcing during forecast	Forecast start date
Short-CTRL	/	7	UKMO (11)	UKMO (11)	Daily forecast starting from 05/01/2015, 05/31/2015, 06/30/2015, 07/30/2015, 08/29/2015, 04/25/2016, 05/25/2016, 06/24/2016, 07/24/2016, 08/23/2016.
Short-SIT	CryoSat-2 SIT	7	UKMO (11)	UKMO (11)	
Short-SIC	SSMI/SSMIS SIC	7	UKMO (11)	UKMO (11)	
Short-SICSIT	SSMI/SSMIS SIC and CryoSat-2 SIT	7	UKMO (11)	UKMO (11)	
Long-CTRL	/	270	ERA5 (1)	CFSv2 (1)	05/16/2015, 06/15/2015, 07/15/2015, 08/14/2015, 09/13/2015, 05/10/2016, 06/09/2016, 07/09/2016, 08/08/2016, 09/07/2016.
Long-SIT	CryoSat-2 SIT	270	ERA5 (1)	CFSv2 (1)	

puted using the NOAA/NSIDC SIC CDR data. The RMSDs of SIT are computed with respect to the CS2SMOS products (Ricker et al., 2017). The SIT observations derived from ULS moorings maintained by the Beaufort Gyre Exploration Program (BGEP) are used for the forecast evaluation. The three moorings BGEP-A, BGEP-B, and BGEP-D, which provide year-round sea-ice draft observations, are located at (75.0°N, 150.0°W), (78.0°N, 150.0°W) and (74.0°N, 140.0°W), respectively (Figure S1). The draft is converted to SIT by multiplying it by a constant factor of 1.1 as in Nguyen et al. (2011).

3 Result

3.1 Short-term ice-edge forecast

An overview of the SIT states of PIOMAS, CryoSat-2, and the short-term experiment assimilation results in 2015 is shown in Figure 1 and in 2016 in Figure S2. In May and June, CryoSat-2 has similar SIT over the compact ice regions but thinner (by more than 0.5 m) ice over the first-year ice regions compared to the PIOMAS SIT. This is more evident in July, August, and September, while the CryoSat-2 SIT is biased low over the central Arctic. Landy et al. (2022) pointed out that the roughness-induced electromagnetic range bias on the heavily-deformed ice in the coast regions north of the CAA and Greenland are responsible for these underestimates. In general, the SIT patterns of CryoSat-2 observations are more similar to the Short-CTRL patterns, which are the extensions of CMST, than to the PIOMAS patterns. Short-CTRL SIT patterns have thinner ice in the Beaufort Sea than the PIOMAS patterns, capturing an expected SIT distribution. This is not surprising since CMST is constructed by assimilating remote-sensed SIT during the freezing season until April (Mu et al., 2018b), while PIOMAS does not assimilate any SIT (J. Zhang & Rothrock, 2003).

The area-averaged SIT differences between Short-SIT and Short-CTRL in May to September of 2015 are 0.10 m, -0.06 m, -0.37 m, -0.37 m and -0.39 m, respectively. Overall, the area-averaged SIT differences are smallest in May and June, when the assimilation of the summer CryoSat-2 observations reduces the SIT in the Amerasian Basin and increases it in the Eurasian Basin. In the strong melt months of July, August and September, when the uncertainties of the CryoSat-2 SIT are at their maximum, the underestimation of the SIT over the multi-year ice regions, i.e., north of the CAA and Greenland, is remarkable. The differences can easily exceed -1 m and even reach -1.5 m. SIT is also reduced in most of the marginal ice zones, especially in the Beaufort Sea and the Chukchi Sea. CMST tends to overestimate late summer SIT in the marginal seas due to unrealistic covariances between SIC and SIT when abrupt increases in SIC are triggered by wind convergences (Mu et al., 2018b). The assimilation of CryoSat-2 SIT corrects this bias, resulting in a more reasonable estimate of SIT in the marginal seas.

SIT assimilation has an important impact on SIC simulations through the physical connection between thickness and concentration (Xie et al., 2016; Mignac et al., 2022). Short-term forecast of ice edge, defined as the 15% SIC isoline, can be strongly influenced by SIT assimilation. Figure 2 shows the reduction of IIEE in the Pacific sector and Atlantic sector (regions shown in Figure S1). IIEE in each forecast experiment is given in Figure S3. The observed SIC used as the reference for the IIEE calculation is the NOAA/NSIDC SIC CDR. The difference in the ice-edge position between forecasts and observations in 2015 and 2016 is displayed in Figure S4 and Figure S5.

The impact of CryoSat-2 SIT assimilation on ice-edge forecasts varies with time and region. Compared to Short-CTRL, IIEE in Short-SIT is strongly reduced in most times and both sectors (Figure 2). In the Pacific sector, the ice-edge position in the forecasts is consistently overestimated in Short-CTRL. Assimilation of the summer SIT reduces the SIT of the forecasts near the ice edge, resulting in a better agreement between the ice-edge forecasts and the ice-edge observations from the satellite (Figure S4 and Figure S5).

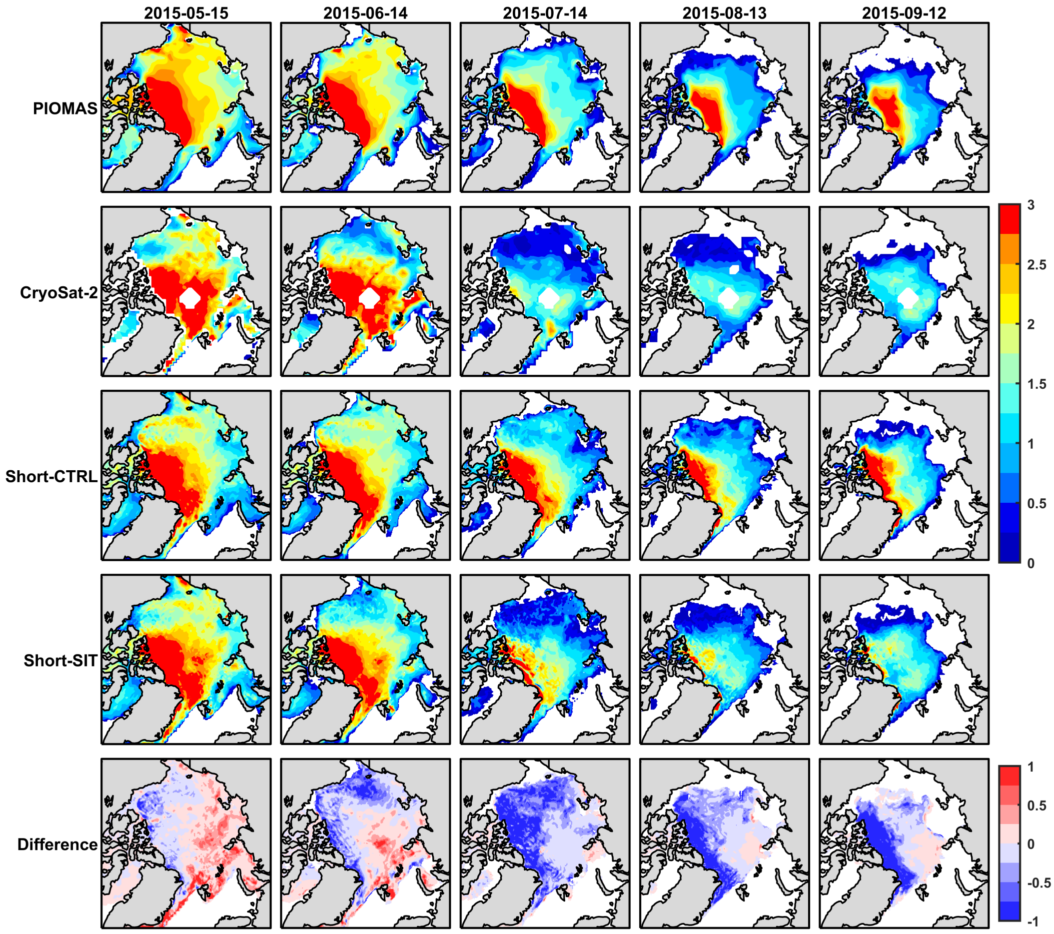

Figure 1. SIT (m) in PIOMAS, CryoSat-2, Short-CTRL, Short-SIT, and the difference between Short-SIT and Short-CTRL 15 days after the start in May to September of 2015. Note that CryoSat-2 observations are two-week averages while the rest are daily SIT.

In May and June, only a slight improvement in IIEE is observed. However, in July, especially in 2015, IIEE increases. This can be attributed to the fact that the melt-pond fraction starts to increase in June and reaches its maximum in July (Feng et al., 2022). In particular, the melt-pond fraction in the Beaufort Sea peaked in 2015 during the 2000-2021 observation period (Xiong & Ren, 2023). The presence of excessive melt-pond fraction may lead to more misclassification of ice leads and melt ponds in the CryoSat-2 sea-ice freeboard retrieval using the CNN model, which affects the SIT analysis in the Pacific sector. Therefore, the underestimated SIT erroneously leads to a large ice-edge error in July of the Short-SIT experiments. This warrants further refinement of the artificial intelligence algorithm used for summer CryoSat-2 SIT retrieval. In late summer, the assimilation of CryoSat-2 SIT observations in Short-SIT leads to more skillful ice-edge forecasts, resulting in a statistically significant average reduction in IIEE of about 2.1×10^5 km^2. For example, the assimilation of SIT allows the model to predict an ice-free "cave" inside the Beaufort Sea in August 2015, while it is completely covered by sea ice in Short-CTRL (Figure S4). Furthermore, the ice-edge forecasts in the Atlantic sector are also improved, especially in June (about 0.8×10^5 km^2) and July (more than 0.9×10^5 km^2).

We further investigate the influences of SIC assimilation together with summer SIT assimilation on the ice-edge forecasts, considering the more important role of SIC observations on summer sea-ice forecasts as documented in the literature (e.g., Posey et al., 2015; Yang, Losa, Losch, Liu, et al., 2015). Forecasts from the Short-SICSIT experiments are also compared to the Short-SIC experiments, which performs SIC assimilation only.

In the Pacific sector, the additional SIT assimilation tends to yield more favorable ice-edge forecasts compared to Short-SIC (Figure 2). Similar to the IIEE differences between Short-SIT and Short-CTRL, the improvement in May and June between Short-SICSIT and Short-SIC is relatively small (only 3.0×10^3 km^2 on average). In July, IIEE becomes smaller in 2015 but larger in 2016 relative to Short-SIC. In late summer, the analysis of summer SIT observations significantly reduces the IIEE, bringing the ice-edge forecasts closer to the observations. In the Atlantic Sector, Short-SICSIT does not yield overwhelmingly better results than Short-SIC (Figure 2). The introduction of summer CryoSat-2 SIT observations gives rise to larger IIEE in May and June, while the IIEE differences are smaller in later months. Nevertheless, these mean IIEE differences are still in the range of $\pm0.5\times10^5$ km^2, which is much smaller than the changes between Short-SIT and Short-CTRL. In the Atlantic sector Short-SIC is already close to the observations due to a reasonable CMST SIT estimate north of the Svalbard and Novaya Zemlya, so further improvements are rather limited.

Note that, as shown by the solid lines representing the mean IIEE differences in Figure 2, the effect of the summer CryoSat-2 SIT assimilation is gradually more evident in most of the months in the Short-SICSIT experiments. The improvements of Short-SICSIT relative to Short-SIC become larger with increasing lead time, while the deteriorations of IIEE become smaller, with the exception of the June 2016 forecasts.

3.2 Long-term sea-ice forecast

The Long-SIT experiments with summer CryoSat-2 SIT assimilation provides significant benefits for ice-edge and thickness forecasts, as shown in Figure 3. Reductions in IIEEs are found in May, June and August in 2015 and in 2016 for the first 30 days (Figure 3a, b). In July, the CryoSat-2 SIT assimilation is only effective for a few days due to the underestimated thickness uncertainties caused by melt ponds. The improvement in ice-edge forecast is also pronounced in September, for three weeks in 2015 and two weeks in 2016: As freezing begins, the IIEE difference gradually increases.

With respect to the CS2SMOS SIT product, the predicted Arctic-wide thickness is also improved (Figure 3c, d), except for the forecast starting in July 2016, which degrades after 140 days. The summer CryoSat-2 SIT mitigates the SIT overestimation in the Beaufort Sea in Long-CTRL that is initialized from the CMST state (not shown). The improvements are most pronounced in October, when the freezing season begins, and decrease exponentially with time until the forecast system falls into the control of the internal variability. This superior skill may even persist throughout the freezing season, similar to the previous findings on an optimal winter SIT initialization improving the predictive skill of summer sea ice (Blockley & Peterson, 2018). Consistent with the performance of the short-term forecasts in section 3.1, the reduction of SIT RMSD in 2015 is more significant than that in 2016, because relatively small SIT difference between summer CryoSat-2 observations and the CMST estimate is observed in 2016.

We also examine the performance of the long-term SIT forecasts at the BGEP sites (Figure S6). In general, significant improvements in the SIT forecasts are found in Long-SIT initialized in July, August and September of 2015. The differences between Long-SIT and Long-CTRL in 2016 are limited, not exceeding 30 cm most of the time. The forecasts tend to overestimate SIT in the early freezing season in the Beaufort Sea. To check if the reason is within the biases of long-term atmospheric forecasts, we performed additional forecast experiments in 2015 (not shown) with the same configuration as Long-CTRL, except that the CFSv2 atmospheric forecast is replaced by the ERA-5 reanalysis for the atmospheric

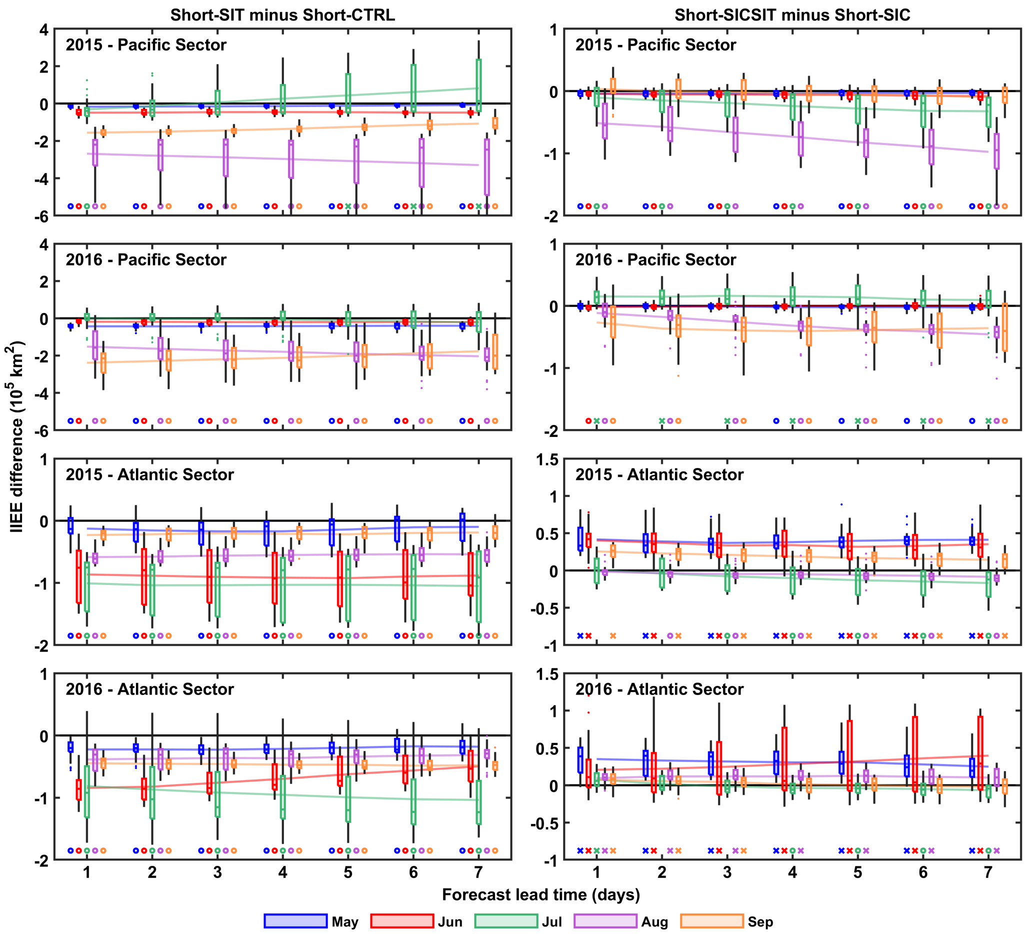

Figure 2. Box plot of the IIEE difference ($10^5 km^2$) between Short-SIT and Short-CTRL (left), together with that between Short-SICSIT and Short-SIC (right) in the 7-day sea-ice forecasts. The IIEE in the box plot is calculated after 7 days of assimilation when the summer CryoSat-2 SIT is fully effective. Blue, red, green, purple and orange boxes indicate different summer months. Colored boxes indicate IIEE difference between the lower and upper quartiles. Colored outliers denote values more than 1.5 interquartile range from the top or bottom of the colored box. The outer edges of the black lines denote the minimum and maximum values that are not outliers. Solid-colored lines show the mean IIEE difference at each lead time. A positive value indicates an increase in IIEE, when SIT is assimilated, while a negative value indicates a decrease in the IIEE. Markers at the bottom of each panel indicate increases (cross) and decreases (circle) in IIEE that pass the Student's T-test at the 95% confidence level. Note that negative values indicate better forecast skills.

forcing. The ERA-5 driven simulations show a similar overestimation of SIT in the Beaufort Sea. The anticyclonic wind in the Beaufort Gyre pushes excessively thick ice from the multi-year ice region north of the CAA into the Beaufort Sea as in Long-CTRL. This suggests that the overestimation is not mainly due to biases in the atmospheric forcing but imperfect model parameterizations and initial ice-ocean conditions.

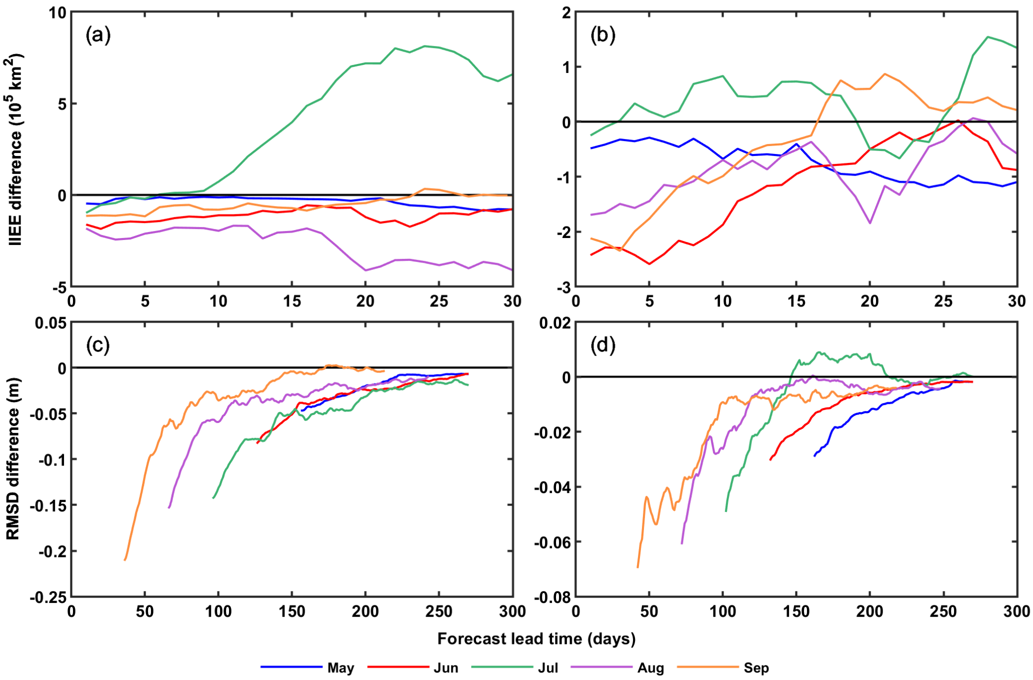

Figure 3. The difference of the IIEE ($10^5 km^2$) in 2015 (a) and in 2016 (b), and the difference of the RMSD of the SIT (m) in 2015 (c) and in 2016 (d) between the Long-SIT and Long-CTRL forecasts initialized from May to September. The RMSD of the SIT is computed with respect to the CS2SMOS product available from October to April, hence the staggered time series in (c) and (d). Note that negative values indicate better forecast skill.

4 Summary

This study examines the impact of summer CryoSat-2 SIT assimilation on short- and long-term sea-ice forecasts in 2015 and in 2016. The ice-edge forecasts with summer CryoSat-2 SIT assimilation are dramatically improved when compared to the experiments without any data assimilation. When the summer CryoSat-2 SIT data are assimilated together with SIC data, the effects on the ice-edge forecast skill are rather dependent on the time when the forecast is initialized and are spatially highly variable. In the Pacific sector, the combined assimilation of summer SIT and SIC observations leads to more realistic summer ice-edge forecasts with a one-week lead time.

The long-term sea-ice forecasts show significant reductions in both IIEE and RMSD of the SIT, except for those initialized in July, when the summer CryoSat-2 SIT has large uncertainties. The improvement in ice-edge forecasts can last up to about 30 days, while for the SIT forecasts the benefits can last for more than 3 months. This result demonstrates that, although the atmospheric forecasts used to drive the model can evolve freely after about one month, the SIT initialization in summer remains a primary factor in predicting long-term SIT variations.

However, limitations of the summer CryoSat-2 SIT data product still remain. The deep learning algorithm used has a certain degree of uncertainty in classifying ice leads and melt ponds, especially when the melt-pond fraction is large. The underestimation in the summer CryoSat-2 SIT from July to September in the coastal regions north of the CAA and Greenland requires further work on the sea-ice freeboard and thickness retrieval algorithm or exploration of new correction schemes to improve their reliability and accuracy. Furthermore, it is still an open question how this product should be used for real-time Arctic sea-ice forecasting, since its uncertainty currently does not account for all the algorithm errors, and possible representation errors (Janjić et al., 2018) should be considered accurately.

5 Open Research

The ensemble mean Arctic sea-ice thickness (SIT) and sea-ice concentration (SIC) forecast data used in the study can be downloaded at Song et al. (2024). The file size of the forecast results with all ensemble members exceeds 50GB and can be made available upon request through contact. The CMST SIT estimate is available at Mu et al. (2018a). The summer CryoSat-2 SIT observations can be downloaded from Landy and Dawson (2022). The SSMI/SSMIS SIC data is avaliable from Kern et al. (2024). The UKMO atmospheric ensemble forecasts are avaliable in the THORPEX Interactive Grand Global Ensemble (TIGGE; Bougeault et al., 2010) archive (`https://apps.ecmwf.int/datasets/data/tigge`). The hourly ERA5 reanalysis is avaliable at Hersbach et al. (2023). The CFSv2 atmospheric forecasts are avaliable at `https://www.ncei.noaa.gov/products/weather-climate-models/climate-forecast-system`. The PIOMAS (J. Zhang & Rothrock, 2003) data is provided at `https://psc.apl.uw.edu/data`. The NOAA/NSIDC SIC CDR data is avaliable at Meier et al. (2021). The CS2SMOS data is avaliable at `https://www.meereisportal.de`. Mooring observations from BGEP are downloaded from `https://www2.whoi.edu/site/beaufortgyre`.

Acknowledgments

This study is supported by the National Key R&D Program of China under Grant 2019YFA0607000, the National Natural Science Foundation of China (42176235) and the Laoshan Laboratory (LSKJ202202300). Contribution of SNL was supported by the Federal Ministry of Education and Research of Germany in the framework of the Seamless Sea Ice Prediction project (SSIP, Grant 01LN1701A) and partly made in the framework of the state assignment of SIO RAS (theme FMWE-2024-0028).

References

Blanchard-Wrigglesworth, E., Bitz, C. M., & Holland, M. M. (2011, 09). Influence of initial conditions and climate forcing on predicting arctic sea ice. *Geophysical Research Letters*, *38*, L18503. doi: 10.1029/2011GL048807

Blockley, E. W., & Peterson, K. A. (2018). Improving met office seasonal predictions of arctic sea ice using assimilation of cryosat-2 thickness. *The Cryosphere*, *12*(11), 3419-3438. doi: 10.5194/tc-12-3419-2018

Bougeault, P., Toth, Z., Bishop, C., Brown, B., Burridge, D., Chen, D. H., … Worley, S. (2010). The thorpex interactive grand global ensemble. *Bulletin of the American Meteorological Society*, *91*(8), 1059-1072. doi: 10.1175/2010BAMS2853.1

Bowler, N. E., Arribas, A., Mylne, K. R., Robertson, K. B., & Beare, S. E. (2008). The mogreps short–range ensemble prediction system. *Quarterly Journal of the Royal Meteorological Society*, *134*(632), 703–722. doi: 10.1002/qj.234

Bushuk, M., Msadek, R., Winton, M., Vecchi, G. A., Gudgel, R., Rosati, A., & Yang, X. (2017). Skillful regional prediction of arctic sea ice on seasonal timescales. *Geophysical Research Letters*, *44*(10), 4953-4964. doi: 10.1002/2017GL073155

Bushuk, M., Winton, M., Bonan, D. B., Blanchard-Wrigglesworth, E., & Delworth, T. L. (2020). A mechanism for the arctic sea ice spring predictability barrier. *Geophysical Research Letters*, *47*(13), e2020GL088335. doi: 10.1029/2020GL088335

Bushuk, M., Zhang, Y., Winton, M., Hurlin, B., Delworth, T., Lu, F., … Zeng, F. (2022, 07). Mechanisms of regional arctic sea ice predictability in two dynamical seasonal forecast systems. *Journal of Climate*, *35*, 4207-4231. doi: 10.1175/JCLI-D-21-0544.1

Comiso, J. C., Parkinson, C. L., Gersten, R., & Stock, L. (2008). Accelerated decline in the arctic sea ice cover. *Geophysical Research Letters*, *35*(1), L01703. doi: 10.1029/2007GL031972

Dawson, G., Landy, J., Tsamados, D. M., Komarov, A. S., Howell, S., Heorton, H., & Krumpen, T. (2022, 01). A 10-year record of arctic summer sea ice freeboard from cryosat-2. *Remote Sensing of Environment*, *268*, 112744. doi: 10.1016/j.rse.2021.112744

Day, J. J., Hawkins, E., & Tietsche, S. (2014). Will arctic sea ice thickness initialization improve seasonal forecast skill? *Geophysical Research Letters*, *41*, 7566-7575. doi: 10.1002/2014GL061694

Day, J. J., Tietsche, S., & Hawkins, E. (2014). Pan-arctic and regional sea ice predictability: initialization month dependence. *Journal of Climate*, *27*(12), 4371-4390. doi: 10.1175/JCLI-D-13-00614.1

Dirkson, A., Merryfield, W. J., & Monahan, A. H. (2017). Impacts of sea ice thickness initialization on seasonal arctic sea ice predictions. *Journal of Climate*, *30*, 1001-1017. doi: 10.1175/JCLI-D-16-0437.1

Drinkwater, M. R. (1991). K $_u$ band airborne radar altimeter observations of marginal sea ice during the 1984 marginal ice zone experiment. *Journal of Geophysical Research: Oceans*, *96*(C3), 4555-4572. doi: 10.1029/90JC01954

Feng, J., Zhang, Y., Cheng, Q., & Tsou, J. Y. (2022). Pan-arctic melt pond fraction trend, variability, and contribution to sea ice changes. *Global and Planetary Change*, *217*, 103932. doi: 10.1016/j.gloplacha.2022.103932

Goessling, H. F., Tietsche, S., Day, J. J., Hawkins, E., & Jung, T. (2016). Predictability of the arctic sea-ice edge. *Geophysical Research Letters*, *43*, 1642–1650. doi: 10.1002/2015GL067232

Guemas, V., Blanchard-Wrigglesworth, E., Chevallier, M., Day, J. J., Déqué, M., Doblas-Reyes, F. J., … Tietsche, S. (2016). A review on arctic sea ice predictability and prediction on seasonal-to-decadal timescales. *Quarterly Journal of the Royal Meteorological Society*, *142*, 546-561. doi: 10.1002/qj.2401

Hebert, D. A., Allard, R. A., Metzger, E. J., Posey, P. G., Preller, R. H., Wallcraft, A. J., … Smedstad, O. M. (2015, 11). Short-term sea ice forecasting: An assessment of ice concentration and ice drift forecasts using the u.s. navy's arctic cap nowcast/forecast system. *Journal of Geophysical Research: Oceans*, *120*, 8327-8345. doi: 10.1002/2015JC011283

Hersbach, H., Bell, B., Berrisford, P., Biavati, G., Horányi, A., Muñoz Sabater, J., … Thépaut, J.-N. (2023). *Era5 hourly data on single levels from 1940 to present* [dataset]. Copernicus Climate Change Service (C3S) Climate Data Store (CDS). Retrieved from `https://cds.climate.copernicus.eu/cdsapp#!/dataset/reanalysis-era5-single-levels?tab=overview` doi: 10.24381/cds.adbb2d47

Hersbach, H., Bell, B., Berrisford, P., Hirahara, S., Horányi, A., Muñoz-Sabater, J., … Thépaut, J.-N. (2020). The era5 global reanalysis. *Quarterly Journal of the Royal Meteorological Society*, 1999–2049. doi: 10.1002/qj.3803

Hibler III, W. D. (1979). A dynamic thermodynamic sea ice model. *Journal of Physical Oceanography*, *9*, 815-846. doi: 10.1175/1520-0485(1979)009<0815:ADTSIM>2.0.CO;2

Janjić, T., Bormann, N., Bocquet, M., Carton, J. A., Cohn, S. E., Dance, S. L., … Weston, P. (2018). On the representation error in data assimilation. *Quarterly Journal of the Royal Meteorological Society*, *144*(713), 1257-1278. doi: 10.1002/qj.3130

Jung, T., Gordon, N. D., Bauer, P., Bromwich, D. H., Chevallier, M., Day, J. J., … Yang, Q. (2016). Advancing polar prediction capabilities on daily to seasonal time scales. *Bulletin of the American Meteorological Society*, *97*, 160113112747009. doi: 10.1175/BAMS-D-14-00246.1

Kaleschke, L., Lüpkes, C., Vilna, T., Haarpaintner, J., Borchert, A., Hartmann, J., & Heygster, G. (2001). Ssm/i sea ice remote sensing for mesoscale ocean-atmosphere interaction analysis. *Canadian Journal of Remote Sensing*, *27*, 526-537. doi: 10.1080/

07038992.2001.10854892

Kern, S., Kaleschke, L., Girard-Ardhuin, F., Spreen, G., & Beitsch, A. (2024). *Global daily gridded 5-day median-filtered, gap-filled asi algorithm ssmi-ssmis sea ice concentration data* [dataset]. Integrated Climate Date Center. Retrieved from `https://www.cen.uni-hamburg.de/en/icdc/data/cryosphere/seaiceconcentration-asi-ssmi.html`

Kern, S., Kaleschke, L., & Spreen, G. (2010). Climatology of the nordic (irminger, greenland, barents, kara and white/pechora) seas ice cover based on 85 ghz satellite microwave radiometry: 1992–2008. *Tellus A*, *62*, 411-434. doi: 10.3402/tellusa.v62i4.15709

Kwok, R., & Rothrock, D. A. (2009). Decline in arctic sea ice thickness from submarine and icesat records: 1958-2008. *Geophysical Research Letters*, *36*, L15501. doi: 10.1029/2009GL039035

Landrum, L., & Holland, M. M. (2020, 12). Extremes become routine in an emerging new arctic. *Nature Climate Change*, *10*, 1-8. doi: 10.1038/s41558-020-0892-z

Landy, J. C., & Dawson, G. J. (2022). *Year-round arctic sea ice thickness from cryosat-2 baseline-d level 1b observations 2010-2020 (version 1.0)* [dataset]. NERC EDS UK Polar Data Centre. Retrieved from `https://data.bas.ac.uk/full-record.php?id=GB/NERC/BAS/PDC/01613` doi: 10.5285/d8c66670-57ad-44fc-8fef-942a46734ecb

Landy, J. C., Dawson, G. J., Tsamados, M., Bushuk, M., Stroeve, J. C., Howell, S. E. L., … Aksenov, Y. (2022). A year-round satellite sea-ice thickness record from cryosat-2. *Nature*, *609*, 1-6. doi: 10.1038/s41586-022-05058-5

Laxon, S. W., Giles, K. A., Ridout, A. L., Wingham, D. J., Willatt, R., Cullen, R., … Davidson, M. (2013). Cryosat-2 estimates of arctic sea ice thickness and volume. *Geophysical Research Letters*, *40*(4), 732-737. doi: 10.1002/grl.50193

Lee, S., Kim, H.-C., & Im, J. (2018). Arctic lead detection using a waveform mixture algorithm from cryosat-2 data. *The Cryosphere*, *12*(5), 1665-1679. doi: 10.5194/tc-12-1665-2018

Lemieux, J.-F., Beaudoin, C., Dupont, F., Roy, F., Smith, G. C., Shlyaeva, A., … Ferry, N. (2015, 03). The regional ice prediction system (rips): Verification of forecast sea ice concentration. *Quarterly Journal of the Royal Meteorological Society*, *142*, 632-643. doi: 10.1002/qj.2526

Losch, M., Menemenlis, D., Campin, J.-M., Heimbach, P., & Hill, C. (2010). On the formulation of sea-ice models. part 1: Effects of different solver implementations and parameterizations. *Ocean Modelling*, *33*(1), 129-144. doi: 10.1016/j.ocemod.2009.12.008

Marshall, J., Adcroft, A., Hill, C., Perelman, L., & Heisey, C. (1997). A finite-volume, incompressible navier stokes model for studies of the ocean on parallel computers. *Journal of Geophysical Research*, *102*, 5753-5766. doi: 10.1029/96JC02775

Maykut, G. A., Grenfell, T. C., & Weeks, W. (1992). On estimating spatial and temporal variations in the properties of ice in the polar oceans. *Journal of Marine Systems*, *3*, 41-72. doi: 10.1016/0924-7963(92)90030-C

Meier, W. N., Fetterer, F., Windnagel, A. K., & Stewart., J. S. (2021). *Noaa/nsidc climate data record of passive microwave sea ice concentration, version 4* [dataset]. National Snow and Ice Data Center. Retrieved from `https://nsidc.org/data/G02202/versions/4` doi: 10.7265/efmz-2t65

Mignac, D., Martin, M., Fiedler, E., Blockley, E., & Fournier, N. (2022, 02). Improving the met office's forecast ocean assimilation model (foam) with the assimilation of satellite-derived sea-ice thickness data from cryosat-2 and smos in the arctic. *Quarterly Journal of the Royal Meteorological Society*, *148*, 1-24. doi: 10.1002/qj.4252

Min, C., Yang, Q., Luo, H., Chen, D., Krumpen, T., Mamnun, N., … Nerger, L. (2023). Improving arctic sea-ice thickness estimates with the assimilation of cryosat-2 summer observations. *Ocean-Land-Atmosphere Research*, *2*, 0025. doi: 10.34133/olar.0025

Mu, L., Liang, X., Yang, Q., Liu, J., & Zheng, F. (2019). Arctic ice ocean prediction system: evaluating sea ice forecasts during xuelong's first trans-arctic passage in summer 2017. *Journal of Glaciology*, 1-9. doi: 10.1017/jog.2019.55

Mu, L., Losch, M., Yang, Q., Ricker, R., Losa, S. N., & Nerger, L. (2018a). *The arc-*

tic combined model and satellite sea ice thickness (cmst) dataset [dataset]. PANGAEA. Retrieved from https://doi.org/10.1594/PANGAEA.891475 doi: 10.1594/PANGAEA.891475

Mu, L., Losch, M., Yang, Q., Ricker, R., Losa, S. N., & Nerger, L. (2018b). Arctic-wide sea ice thickness estimates from combining satellite remote sensing data and a dynamic ice-ocean model with data assimilation during the cryosat-2 period. *Journal of Geophysical Research: Oceans*, *123*, 7763-7780. doi: 10.1029/2018JC014316

Mu, L., Nerger, L., Streffing, J., Tang, Q., Niraula, B., Zampieri, L., … Goessling, H. F. (2022). Sea-ice forecasts with an upgraded awi coupled prediction system. *Journal of Advances in Modeling Earth Systems*, *14*(12), e2022MS003176. doi: 10.1029/2022MS003176

Mu, L., Yang, Q., Losch, M., Losa, S. N., Ricker, R., Nerger, L., & Liang, X. (2017). Improving sea ice thickness estimates by assimilating cryosat-2 and smos sea ice thickness data simultaneously: Cryosat-2 and smos sea ice thickness data assimilation. *Quarterly Journal of the Royal Meteorological Society*, *144*, 529-538. doi: 10.1002/qj.3225

Nerger, L., Hibler III, W. D., & SCHRÖTER, J. (2005). Pdaf-the parallel data assimilation framework: Experiences with kalman filtering. *World Scientific*, 63–83. doi: 10.1142/9789812701831_0006

Nerger, L., Janjić, T., Schröter, J., & Hiller, W. (2012). A regulated localization scheme for ensemble-based kalman filters. *Quarterly Journal of the Royal Meteorological Society*, *138*(664), 802-812. doi: 10.1002/qj.945

Nguyen, A. T., Menemenlis, D., & Kwok, R. (2011). Arctic ice-ocean simulation with optimized model parameters: Approach and assessment. *Journal of Geophysical Research: Oceans*, *116*, C04025. doi: 10.1029/2010JC006573

Parkinson, C. L., & Washington, W. M. (1979). A large-scale numerical model of sea ice. *Journal of Geophysical Research*, *84*, 311-337. doi: 10.1029/JC084iC01p00311

Posey, P., Metzger, E., Wallcraft, A., Hebert, D., Allard, R., Smedstad, O., … Helfrich, S. (2015, 08). Improving arctic sea ice edge forecasts by assimilating high horizontal resolution sea ice concentration data into the us navy's ice forecast systems. *The Cryosphere*, *9*, 1735-1745. doi: 10.5194/tc-9-1735-2015

Ricker, R., Hendricks, S., Helm, V., Skourup, H., & Davidson, M. (2014). Sensitivity of cryosat-2 arctic sea-ice freeboard and thickness on radar-waveform interpretation. *The Cryosphere*, *8*, 1607-1622. doi: 10.5194/tc-8-1607-2014

Ricker, R., Hendricks, S., Kaleschke, L., Tian-Kunze, X., King, J., & Haas, C. (2017). A weekly arctic sea-ice thickness data record from merged cryosat-2 and smos satellite data. *The Cryosphere*, *11*(4), 1607–1623. doi: 10.5194/tc-11-1607-2017

Rothrock, D. A., Yu, Y., & Maykut, G. A. (1999). Thinning of the arctic sea-ice cover. *Geophysical Research Letters*, *26*, 3469-3472. doi: 10.1029/1999GL010863

Saha, S., Moorthi, S., Wu, X., Wang, J., Nadiga, S., Tripp, P., … Becker, E. (2014). The ncep climate forecast system version 2. *Journal of Climate*, *27*, 2185–2208. doi: 10.1175/JCLI-D-12-00823.1

Schlitzer, R. (2023). *Ocean data view* [software]. Retrieved from https://odv.awi.de

Semtner, A. J. (1976). A model for thermodynamic growth of sea ice in numerical investigations if climate. *Journal of Physical Oceanography*, *6*, 379-389. doi: 10.1175/1520-0485(1976)006<0379:AMFTTG>2.0.CO;2

Shu, Q., Qiao, F., Liu, J., Song, Z., Chen, Z., Zhao, J., … Song, Y. (2021). Arctic sea ice concentration and thickness data assimilation in the fio-esm climate forecast system. *Acta Oceanologica Sinica*, *40*, 65-75. doi: 10.1007/s13131-021-1768-4

Song, R., Mu, L., Kauker, F., Loza, S., & Chen, X. (2024). *Forecast data for the paper: "assimilating summer sea-ice thickness observations improves arctic sea-ice forecast"* [dataset]. Zenodo. Retrieved from https://doi.org/10.5281/zenodo.10589315 doi: 10.5281/zenodo.10589315

Spreen, G., Kaleschke, L., & Heygster, G. (2008). Sea ice remote sensing using amsr-e 89-ghz channels. *Journal of Geophysical Research*, *113*, C02S03. doi: 10.1029/2005JC003384

Stroeve, J. C., Serreze, M. C., Holland, M. M., Kay, J. E., Malanik, J., & Barrett, A. P.

(2012, 02). The arctic's rapidly shrinking sea ice cover: A research synthesis. *Climatic Change*, *110*, 1005-1027. doi: 10.1007/s10584-011-0101-1

Tilling, R., Ridout, A., & Shepherd, A. (2019). Assessing the impact of lead and floe sampling on arctic sea ice thickness estimates from envisat and cryosat-2. *Journal of Geophysical Research: Oceans*, *124*, 7473–7485. doi: 10.1029/2019JC015232

Xie, J., Counillon, F., Bertino, L., Tian-Kunze, X., & Kaleschke, L. (2016). Benefits of assimilating thin sea ice thickness from smos into the topaz system. *The Cryosphere*, *10*, 2745–2761. doi: 10.5194/tc-10-2745-2016

Xiong, C., & Ren, Y. (2023). Arctic sea ice melt pond fraction in 2000–2021 derived by dynamic pixel spectral unmixing of modis images. *ISPRS Journal of Photogrammetry and Remote Sensing*, *197*, 181-198. doi: 10.1016/j.isprsjprs.2023.01.023

Yang, Q., Losa, S. N., Losch, M., Jung, T., & Nerger, L. (2015). The role of atmospheric uncertainty in arctic summer sea ice data assimilation and prediction. *Quarterly Journal of the Royal Meteorological Society*, *141*, 2314-2323. doi: 10.1002/qj.2523

Yang, Q., Losa, S. N., Losch, M., Liu, J., Zhang, Z., Nerger, L., & Yang, H. (2015). Assimilating summer sea-ice concentration into a coupled ice–ocean model using a lseik filter. *Annals of Glaciology*, *56*(69), 38–44. doi: 10.3189/2015AoG69A740

Yang, Q., Losch, M., Losa, S. N., Jung, T., Nerger, L., & Lavergne, T. (2016). Brief communication: The challenge and benefit of using sea ice concentration satellite data products with uncertainty estimates in summer sea ice data assimilation. *The Cryosphere*, *10*, 761-774. doi: 10.5194/tc-10-761-2016

Zhang, J., & Hibler III, W. D. (1997). On an efficient numerical method for modeling sea ice dynamics. *Journal of Geophysical Research*, *102*, 8691–8702. doi: 10.1029/96JC03744

Zhang, J., & Rothrock, D. A. (2003). Modeling global sea ice with a thickness and enthalpy distribution model in generalized curvilinear coordinates. *Monthly Weather Review*, *131*, 845–861. doi: 10.1175/1520-0493(2003)131<0845:MGSIWA>2.0.CO;2

Zhang, Y.-F., Bushuk, M., Winton, M., Hurlin, B., Gregory, W., Landy, J., & Jia, L. (2023). Improvements in september arctic sea ice predictions via assimilation of summer cryosat-2 sea ice thickness observations. *Geophysical Research Letters*, *50*(24), e2023GL105672. doi: 10.1029/2023GL105672

Assimilating summer sea-ice thickness observations improves Arctic sea-ice forecast

Ruizhe Song[1,2,3,4], Longjiang Mu[2], Svetlana N. Loza[3,5], Frank Kauker[3], Xianyao Chen[1,2]

[1]Frontier Science Center for Deep Ocean Multispheres and Earth System and Physical Oceanography Laboratory, Ocean University of China, Qingdao, China
[2]Laoshan Laboratory, Qingdao, China
[3]Alfred Wegener Institute, Helmholtz Centre for Polar and Marine Research, Bremerhaven, Germany
[4]Academy of the Future Ocean, Ocean University of China, Qingdao, China
[5]Shirshov Institute of Oceanology, Russian Academy of Sciences, Moscow, Russia

Key Points:

- Assimilating summer CryoSat-2 sea-ice thickness (SIT) observations makes more skillful Arctic ice-edge forecasts on multiple time scales.
- The long-term SIT forecasts improve with the assimilation of summer CryoSat-2 SIT observations.
- Further refinement is needed for summer CryoSat-2 SIT observations.

Corresponding author: Longjiang Mu, `ljmu@qnlm.ac`

Abstract

Proper Arctic sea-ice forecasting for the melt season is still a major challenge because of the recent lack of reliable pan-Arctic summer sea-ice thickness (SIT) data. A new summer CryoSat-2 SIT observation data set based on an artificial intelligence algorithm may alleviate this situation. We assess the impact of this new data set on the initialization of sea-ice forecasts in the melt seasons of 2015 and 2016 in a coupled sea ice-ocean model with data assimilation. We find that the assimilation of the summer CryoSat-2 SIT observations can reduce the summer ice-edge forecast error. Further, adding SIT observations to an established forecast system with sea-ice concentration assimilation leads to more realistic short-term summer ice-edge forecasts in the Arctic Pacific sector. The long-term Arctic-wide SIT prediction is also improved. In spite of remaining uncertainties, summer CryoSat-2 SIT observations have the potential to improve Arctic sea-ice forecast on multiple time scales.

Plain Language Summary

Arctic sea ice is rapidly declining due to global warming, especially in summer. Accurate sea-ice forecasting is important to understand the potential influence of these changes and devise effective responses. The performance of sea-ice forecasts highly depends on the accuracy of the initial sea-ice states. So refining the initial conditions of sea-ice forecasts with satellite observations is a common way to reduce forecast errors. However, obtaining reliable summer pan-Arctic satellite sea-ice thickness (SIT) data is challenging due to complex ice-surface conditions in summer. A new artificial-intelligence-based summer SIT satellite data product may mitigate this situation. We integrate this data set into a sea-ice forecast system to evaluate its impact on forecast accuracy. We find that the new summer satellite SIT data can reduce short-term ice-edge location forecast errors and benefit long-term SIT forecasts.

1 Introduction

Arctic sea ice is declining at unprecedented speed (Rothrock et al., 1999; Comiso et al., 2008; Kwok & Rothrock, 2009; Stroeve et al., 2012), which would pose challenges to climatic and ecological stakeholders (Landrum & Holland, 2020). The Arctic Passage, opening up with the gradually melting summer sea ice, calls for accurate Arctic sea-ice prediction from daily to seasonal scales (Jung et al., 2016).

Accurate initialization of sea-ice state is vital for predicting Arctic sea ice (e.g., Blanchard-Wrigglesworth et al., 2011; Guemas et al., 2016; Xie et al., 2016; Dirkson et al., 2017; Bushuk et al., 2022). The assimilation of sea-ice concentration (SIC) has improved the short-term sea-ice forecasts greatly as documented in the literature, and is now widely used at forecasting centers (e.g., Hebert et al., 2015; Lemieux et al., 2015). Sea-ice thickness (SIT) persists longer, therefore assimilation of SIT raises long-term sea-ice forecast skills even stronger (Day, Hawkins, & Tietsche, 2014; Shu et al., 2021; Mu et al., 2022).

However, the potential impacts of summer SIT observations on sea-ice forecasts are not examined comprehensively yet due to a lack of data. An effective retrieval method for the remotely sensed SIT from May to September was missing (Laxon et al., 2013; Ricker et al., 2014). The complex summer ice-surface conditions restrict the application of classical algorithms designed for winter conditions. For instance, melt ponds which occupy a huge fraction of the sea-ice surface in the melt seasons (Maykut et al., 1992) complicate the classification algorithms (Lee et al., 2018; Tilling et al., 2019) and introduce large uncertainties due to increased moisture in the snow (Drinkwater, 1991). On the other hand, in-situ Arctic SIT observations are rather scarce and localized. They can hardly be used in basin-scale assimilation systems.

In a recent study, Dawson et al. (2022) presented the first estimate of pan-Arctic summer sea-ice freeboard from radar altimeter by using a 1D convolutional neural network (CNN) to distinguish ice leads from melt ponds. Landy et al. (2022) converted summer CryoSat-2 radar freeboard to SIT and applied further corrections. The spring predictability barrier of the Arctic sea ice (e.g., Day, Tietsche, & Hawkins, 2014; Bushuk et al., 2017) suggests that sea-ice forecast should benefit from the initialization with SIT in the melt season (Bushuk et al., 2020). Therefore, it presents an opportunity to explore the extent to which the summer SIT observation could improve the real-time forecast skill. Min et al. (2023) demonstrated that assimilation of summer SIT corrects the overestimation in the Combined Model and Satellite Thickness (CMST; Mu et al., 2018b) product. Y.-F. Zhang et al. (2023) found that the assimilation of May to August CryoSat-2 SIT anomalies improves local SIC and sea-ice extent (SIE) forecasts in September. However, the influence of assimilating summer CryoSat-2 SIT observations on short-term sea-ice forecast in summer and on long-term forecast extending beyond September still needs to be investigated further.

In this study, we focus on the impact of summer SIT observations on the daily and seasonal forecast skills of a sea-ice prediction modelling system. In particular, we perform a series of short- and long-term ensemble sea-ice forecasts where the sea ice-ocean initial state is constrained by the summer CryoSat-2 SIT or where these data are not used. The benefits and challenges of using these new SIT data are evaluated and critically discussed using independent sea-ice data.

2 Data and Methods

2.1 The coupled sea ice-ocean model

We use a regional coupled sea ice-ocean model driven by atmospheric forecasts to configure the sea ice-ocean forecast system. The model is based on the Massachusetts Institute of Technology general circulation model (MITgcm; Marshall et al., 1997) and covers the pan-Arctic region with a horizontal resolution of around 18 km as in Losch et al. (2010). The sea-ice model uses a viscous-plastic rheology (Hibler III, 1979; J. Zhang & Hibler III, 1997) and a so called zero-layer thermodynamic formulation without heat capacity (Semtner, 1976; Parkinson & Washington, 1979). The readers are referred to Losch et al. (2010) and Nguyen et al. (2011) for more details on the model.

2.2 Data assimilation and forecast

The summer data assimilation system is initialized from restart files generated by CMST (Mu et al., 2018b) simulation with 11 ensemble members. CMST combines model physics with information from remote-sensed SIT and SIC observations. It successfully reproduces the spatio-temporal sea-ice variations (Mu et al., 2018b). The summer data assimilation and forecast strategy follows Mu et al. (2017) and Mu et al. (2019). A Local Error Subspace Transform Kalman Filter (Nerger et al., 2012) coded within the Parallel Data Assimilation Framework (Nerger et al., 2005) is used to assimilate the summer SIT and SIC observations separately or simultaneously. Then, the summer ensemble forecasts start from the new individual analyses and the model is integrated forced by the atmospheric forecasts (cf. Section 2.3).

The CryoSat-2 summer SIT data set is derived from local variations in the CryoSat-2 radar echo response using a deep learning method (Dawson et al., 2022; Landy et al., 2022). This is the first estimate of pan-Arctic summer SIT from satellite observations. However, the accuracy of the CryoSat-2 summer SIT still needs to be further improved after the correction introduced by Landy et al. (2022), for example over the regions north of the Greenland and the Canadian Arctic Archipelago (CAA). The summer SIT is assimilated into the system on a daily basis using the observations linearly interpolated between two biweekly records. Considering the shortcomings of the summer SIT over thick ice regions, practical experience suggests that the observation uncertainties should be set higher than the original values over thick ice regions, while still using the provided errors over thin ice regions (Supporting Information). The SIC data used in the assimilation are computed at the French Research Institute for Exploitation of the Sea (IFREMER) based on the 85-GHz SSM/I and SSM/IS channels (Kaleschke et al., 2001; Spreen et al., 2008; Kern et al., 2010). The uncertainty of the SIC observation is set to a constant value of 0.25 following Yang, Losa, Losch, Jung, and Nerger (2015) and Yang et al. (2016).

The short-term ensemble assimilation and forecast experiments are driven by the 174-hour atmospheric ensemble forecasts from the United Kingdom Met Office (UKMO) Ensemble Prediction System (EPS; Bowler et al., 2008). For the long-term prediction, the ensemble members are driven by deterministic atmospheric forcing (single member). The hourly European Centre for Medium-Range Weather Forecasts Reanalysis v5 (ERA-5; Hersbach et al., 2020) is used as the atmospheric forcing during the data assimilation, while the atmospheric forecasts from the National Center for Environmental Prediction Climate Forecast System Version 2 (CFSv2; Saha et al., 2014) are used for the 9-month long-term forecasts.

2.3 Experiment design

In order to investigate the potential impact of the CryoSat-2 summer SIT on sea-ice forecasts, this study designs both short-term (7 days) and long-term (270 days) forecasts (Table. 1). These experiments are conducted over different months. The short-term experiments in 2015, which cover the melt season, start from the CMST restart files on May 1, May 31, June 30, July 30, and August 29, respectively. Each forecast experiment lasts for 30 days and on each day a 7-day sea-ice forecast is run using the atmospheric forcing from the daily UKMO ensemble forecasts. No data assimilation is applied in the control run of the short-term forecasts (Short-CTRL). The Short-SIT experiments assimilate only the CryoSat-2 summer SIT data, and the Short-SIC experiments assimilate only the SSMI/SSMIS SIC data, while both data sets are assimilated in the Short-SICSIT experiments. For the 2016 experiments, only the start dates are changed to match the available restart files from CMST (Table. 1).

The long-term forecast experiments are designed to diagnose the persistence of the assimilated CryoSat-2 summer SIT over the months from the melt season to the freezing season. The Long-SIT experiments with SIT assimilation start each summer month from CMST restart files and a daily data assimilation step iterating over 15 days is performed to mitigate abrupt SIT changes. Over that period, ERA5 atmospheric reanalysis forcing is used. Then, the 270-day sea-ice forecasts start from the sea-ice analysis restart files and are forced by the CFSv2 operational atmospheric forecasts. No data assimilation is performed in the Long-CTRL experiments. The forecast start dates are listed in Table 1.

2.4 Verification

Simulation output from the Pan-Arctic Ice-Ocean Modeling and Assimilation System (PIOMAS; J. Zhang & Rothrock, 2003) is employed for the comparison with the assimilation results. PIOMAS is constrained by SIC and sea surface temperature observations. Its modeled SIT has been validated to be comparable to in-situ observations and has been widely used in previous studies.

The integrated ice-edge error (IIEE; Goessling et al., 2016) is used to quantify the skill of the short-term ice-edge forecasts. It measures the discrepancy between the forecasted and observed SIE. The reference observation used in this study is the NOAA/NSIDC Climate Data Record (CDR) of Passive Microwave Sea Ice Concentration Version 4 (Meier et al., 2021).

To validate the skill of the long-term sea-ice forecast, we compute the IIEE and the RMSD of SIT against various other products and in-situ observations. The IIEE is com-

Table 1. Summary of forecast experiments design. Short: short-term forecast. Long: long-term forecast.

Experiment	Assimilated data	Forecast duration (days)	Atmospheric forcing during assimilation	Atmospheric forcing during forecast	Forecast start date
Short-CTRL	/	7	UKMO (11)	UKMO (11)	Daily forecast starting from 05/01/2015, 05/31/2015, 06/30/2015, 07/30/2015, 08/29/2015, 04/25/2016, 05/25/2016, 06/24/2016, 07/24/2016, 08/23/2016.
Short-SIT	CryoSat-2 SIT	7	UKMO (11)	UKMO (11)	
Short-SIC	SSMI/SSMIS SIC	7	UKMO (11)	UKMO (11)	
Short-SICSIT	SSMI/SSMIS SIC and CryoSat-2 SIT	7	UKMO (11)	UKMO (11)	
Long-CTRL	/	270	ERA5 (1)	CFSv2 (1)	05/16/2015, 06/15/2015, 07/15/2015, 08/14/2015, 09/13/2015, 05/10/2016, 06/09/2016, 07/09/2016, 08/08/2016, 09/07/2016.
Long-SIT	CryoSat-2 SIT	270	ERA5 (1)	CFSv2 (1)	

puted using the NOAA/NSIDC SIC CDR data. The RMSDs of SIT are computed with respect to the CS2SMOS products (Ricker et al., 2017). The SIT observations derived from ULS moorings maintained by the Beaufort Gyre Exploration Program (BGEP) are used for the forecast evaluation. The three moorings BGEP-A, BGEP-B, and BGEP-D, which provide year-round sea-ice draft observations, are located at (75.0°N, 150.0°W), (78.0°N, 150.0°W) and (74.0°N, 140.0°W), respectively (Figure S1). The draft is converted to SIT by multiplying it by a constant factor of 1.1 as in Nguyen et al. (2011).

3 Result

3.1 Short-term ice-edge forecast

An overview of the SIT states of PIOMAS, CryoSat-2, and the short-term experiment assimilation results in 2015 is shown in Figure 1 and in 2016 in Figure S2. In May and June, CryoSat-2 has similar SIT over the compact ice regions but thinner (by more than 0.5 m) ice over the first-year ice regions compared to the PIOMAS SIT. This is more evident in July, August, and September, while the CryoSat-2 SIT is biased low over the central Arctic. Landy et al. (2022) pointed out that the roughness-induced electromagnetic range bias on the heavily-deformed ice in the coast regions north of the CAA and Greenland are responsible for these underestimates. In general, the SIT patterns of CryoSat-2 observations are more similar to the Short-CTRL patterns, which are the extensions of CMST, than to the PIOMAS patterns. Short-CTRL SIT patterns have thinner ice in the Beaufort Sea than the PIOMAS patterns, capturing an expected SIT distribution. This is not surprising since CMST is constructed by assimilating remote-sensed SIT during the freezing season until April (Mu et al., 2018b), while PIOMAS does not assimilate any SIT (J. Zhang & Rothrock, 2003).

The area-averaged SIT differences between Short-SIT and Short-CTRL in May to September of 2015 are 0.10 m, -0.06 m, -0.37 m, -0.37 m and -0.39 m, respectively. Overall, the area-averaged SIT differences are smallest in May and June, when the assimilation of the summer CryoSat-2 observations reduces the SIT in the Amerasian Basin and increases it in the Eurasian Basin. In the strong melt months of July, August and September, when the uncertainties of the CryoSat-2 SIT are at their maximum, the underestimation of the SIT over the multi-year ice regions, i.e., north of the CAA and Greenland, is remarkable. The differences can easily exceed -1 m and even reach -1.5 m. SIT is also reduced in most of the marginal ice zones, especially in the Beaufort Sea and the Chukchi Sea. CMST tends to overestimate late summer SIT in the marginal seas due to unrealistic covariances between SIC and SIT when abrupt increases in SIC are triggered by wind convergences (Mu et al., 2018b). The assimilation of CryoSat-2 SIT corrects this bias, resulting in a more reasonable estimate of SIT in the marginal seas.

SIT assimilation has an important impact on SIC simulations through the physical connection between thickness and concentration (Xie et al., 2016; Mignac et al., 2022). Short-term forecast of ice edge, defined as the 15% SIC isoline, can be strongly influenced by SIT assimilation. Figure 2 shows the reduction of IIEE in the Pacific sector and Atlantic sector (regions shown in Figure S1). IIEE in each forecast experiment is given in Figure S3. The observed SIC used as the reference for the IIEE calculation is the NOAA/NSIDC SIC CDR. The difference in the ice-edge position between forecasts and observations in 2015 and 2016 is displayed in Figure S4 and Figure S5.

The impact of CryoSat-2 SIT assimilation on ice-edge forecasts varies with time and region. Compared to Short-CTRL, IIEE in Short-SIT is strongly reduced in most times and both sectors (Figure 2). In the Pacific sector, the ice-edge position in the forecasts is consistently overestimated in Short-CTRL. Assimilation of the summer SIT reduces the SIT of the forecasts near the ice edge, resulting in a better agreement between the ice-edge forecasts and the ice-edge observations from the satellite (Figure S4 and Figure S5).

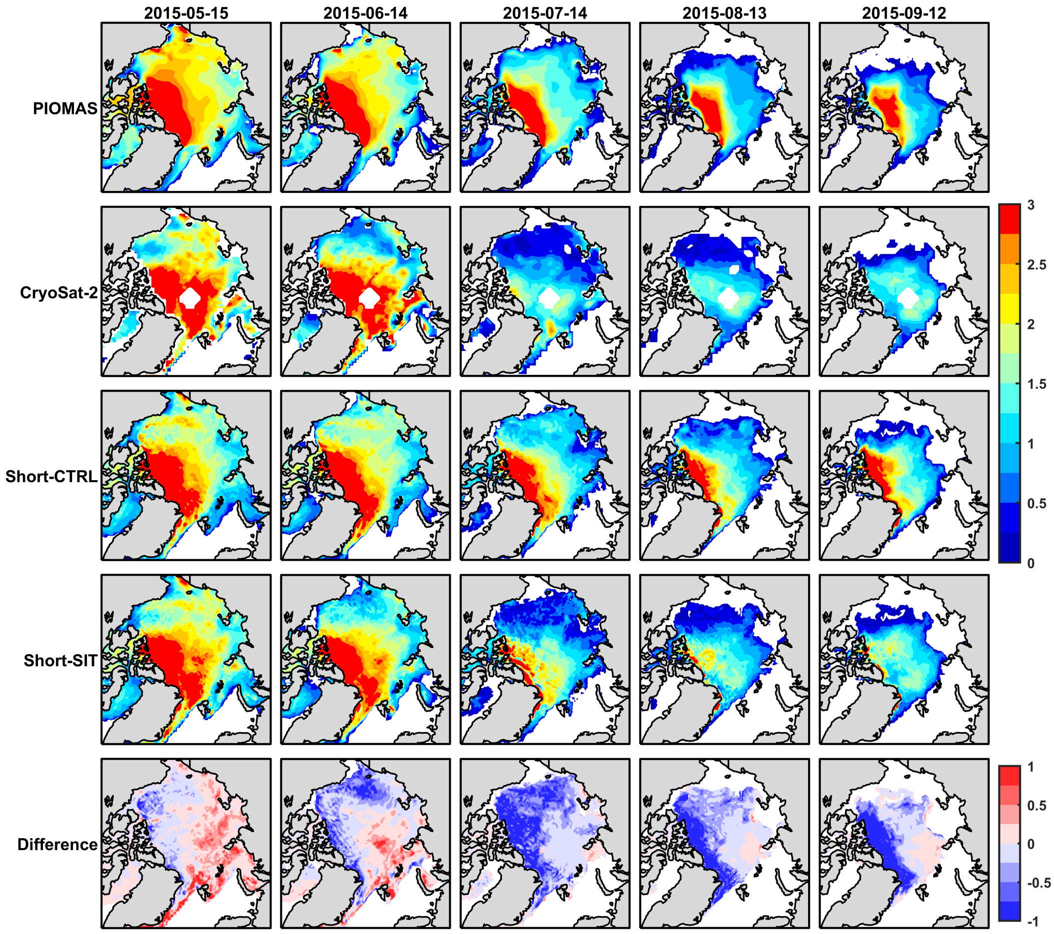

Figure 1. SIT (m) in PIOMAS, CryoSat-2, Short-CTRL, Short-SIT, and the difference between Short-SIT and Short-CTRL 15 days after the start in May to September of 2015. Note that CryoSat-2 observations are two-week averages while the rest are daily SIT.

In May and June, only a slight improvement in IIEE is observed. However, in July, especially in 2015, IIEE increases. This can be attributed to the fact that the melt-pond fraction starts to increase in June and reaches its maximum in July (Feng et al., 2022). In particular, the melt-pond fraction in the Beaufort Sea peaked in 2015 during the 2000-2021 observation period (Xiong & Ren, 2023). The presence of excessive melt-pond fraction may lead to more misclassification of ice leads and melt ponds in the CryoSat-2 sea-ice freeboard retrieval using the CNN model, which affects the SIT analysis in the Pacific sector. Therefore, the underestimated SIT erroneously leads to a large ice-edge error in July of the Short-SIT experiments. This warrants further refinement of the artificial intelligence algorithm used for summer CryoSat-2 SIT retrieval. In late summer, the assimilation of CryoSat-2 SIT observations in Short-SIT leads to more skillful ice-edge forecasts, resulting in a statistically significant average reduction in IIEE of about 2.1×10^5 km^2. For example, the assimilation of SIT allows the model to predict an ice-free "cave" inside the Beaufort Sea in August 2015, while it is completely covered by sea ice in Short-CTRL (Figure S4). Furthermore, the ice-edge forecasts in the Atlantic sector are also improved, especially in June (about 0.8×10^5 km^2) and July (more than 0.9×10^5 km^2).

We further investigate the influences of SIC assimilation together with summer SIT assimilation on the ice-edge forecasts, considering the more important role of SIC observations on summer sea-ice forecasts as documented in the literature (e.g., Posey et al., 2015; Yang, Losa, Losch, Liu, et al., 2015). Forecasts from the Short-SICSIT experiments are also compared to the Short-SIC experiments, which performs SIC assimilation only.

In the Pacific sector, the additional SIT assimilation tends to yield more favorable ice-edge forecasts compared to Short-SIC (Figure 2). Similar to the IIEE differences between Short-SIT and Short-CTRL, the improvement in May and June between Short-SICSIT and Short-SIC is relatively small (only 3.0×10^3 km^2 on average). In July, IIEE becomes smaller in 2015 but larger in 2016 relative to Short-SIC. In late summer, the analysis of summer SIT observations significantly reduces the IIEE, bringing the ice-edge forecasts closer to the observations. In the Atlantic Sector, Short-SICSIT does not yield overwhelmingly better results than Short-SIC (Figure 2). The introduction of summer CryoSat-2 SIT observations gives rise to larger IIEE in May and June, while the IIEE differences are smaller in later months. Nevertheless, these mean IIEE differences are still in the range of $\pm0.5\times10^5$ km^2, which is much smaller than the changes between Short-SIT and Short-CTRL. In the Atlantic sector Short-SIC is already close to the observations due to a reasonable CMST SIT estimate north of the Svalbard and Novaya Zemlya, so further improvements are rather limited.

Note that, as shown by the solid lines representing the mean IIEE differences in Figure 2, the effect of the summer CryoSat-2 SIT assimilation is gradually more evident in most of the months in the Short-SICSIT experiments. The improvements of Short-SICSIT relative to Short-SIC become larger with increasing lead time, while the deteriorations of IIEE become smaller, with the exception of the June 2016 forecasts.

3.2 Long-term sea-ice forecast

The Long-SIT experiments with summer CryoSat-2 SIT assimilation provides significant benefits for ice-edge and thickness forecasts, as shown in Figure 3. Reductions in IIEEs are found in May, June and August in 2015 and in 2016 for the first 30 days (Figure 3a, b). In July, the CryoSat-2 SIT assimilation is only effective for a few days due to the underestimated thickness uncertainties caused by melt ponds. The improvement in ice-edge forecast is also pronounced in September, for three weeks in 2015 and two weeks in 2016: As freezing begins, the IIEE difference gradually increases.

With respect to the CS2SMOS SIT product, the predicted Arctic-wide thickness is also improved (Figure 3c, d), except for the forecast starting in July 2016, which degrades after 140 days. The summer CryoSat-2 SIT mitigates the SIT overestimation in the Beaufort Sea in Long-CTRL that is initialized from the CMST state (not shown). The improvements are most pronounced in October, when the freezing season begins, and decrease exponentially with time until the forecast system falls into the control of the internal variability. This superior skill may even persist throughout the freezing season, similar to the previous findings on an optimal winter SIT initialization improving the predictive skill of summer sea ice (Blockley & Peterson, 2018). Consistent with the performance of the short-term forecasts in section 3.1, the reduction of SIT RMSD in 2015 is more significant than that in 2016, because relatively small SIT difference between summer CryoSat-2 observations and the CMST estimate is observed in 2016.

We also examine the performance of the long-term SIT forecasts at the BGEP sites (Figure S6). In general, significant improvements in the SIT forecasts are found in Long-SIT initialized in July, August and September of 2015. The differences between Long-SIT and Long-CTRL in 2016 are limited, not exceeding 30 cm most of the time. The forecasts tend to overestimate SIT in the early freezing season in the Beaufort Sea. To check if the reason is within the biases of long-term atmospheric forecasts, we performed additional forecast experiments in 2015 (not shown) with the same configuration as Long-CTRL, except that the CFSv2 atmospheric forecast is replaced by the ERA-5 reanalysis for the atmospheric

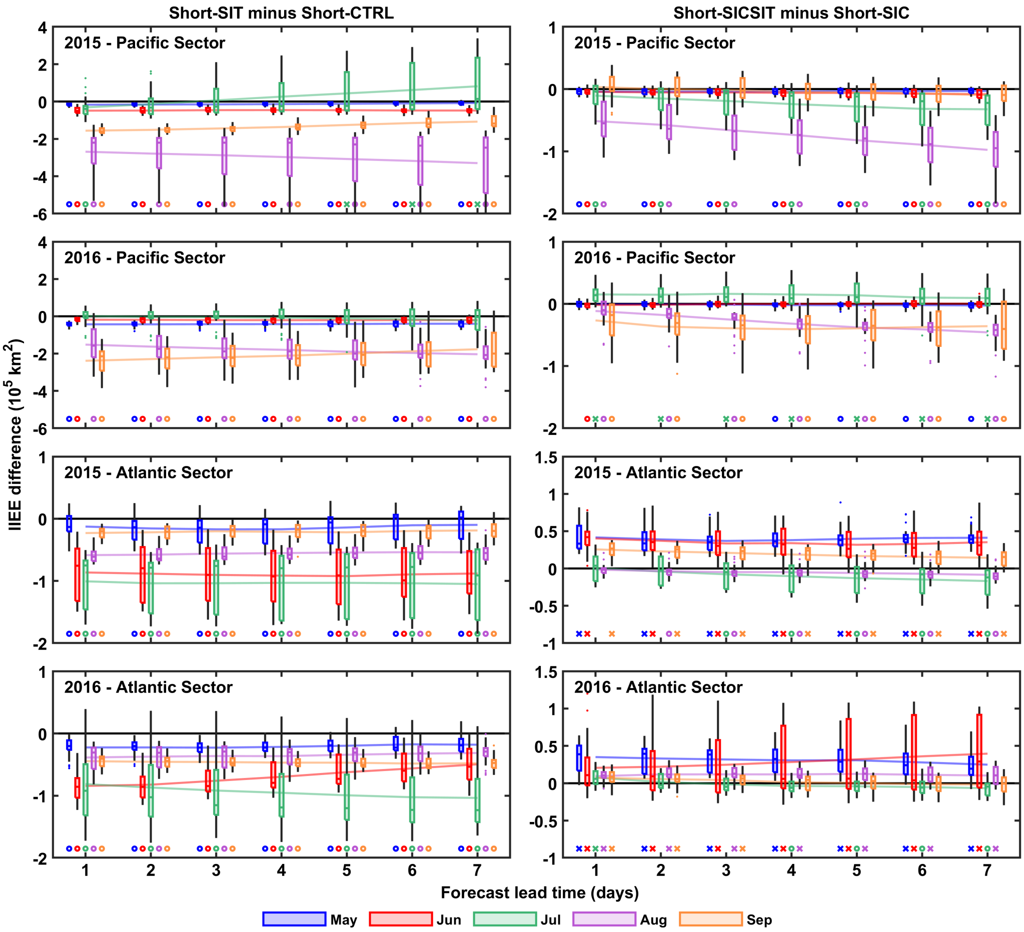

Figure 2. Box plot of the IIEE difference ($10^5 km^2$) between Short-SIT and Short-CTRL (left), together with that between Short-SICSIT and Short-SIC (right) in the 7-day sea-ice forecasts. The IIEE in the box plot is calculated after 7 days of assimilation when the summer CryoSat-2 SIT is fully effective. Blue, red, green, purple and orange boxes indicate different summer months. Colored boxes indicate IIEE difference between the lower and upper quartiles. Colored outliers denote values more than 1.5 interquartile range from the top or bottom of the colored box. The outer edges of the black lines denote the minimum and maximum values that are not outliers. Solid-colored lines show the mean IIEE difference at each lead time. A positive value indicates an increase in IIEE, when SIT is assimilated, while a negative value indicates a decrease in the IIEE. Markers at the bottom of each panel indicate increases (cross) and decreases (circle) in IIEE that pass the Student's T-test at the 95% confidence level. Note that negative values indicate better forecast skills.

forcing. The ERA-5 driven simulations show a similar overestimation of SIT in the Beaufort Sea. The anticyclonic wind in the Beaufort Gyre pushes excessively thick ice from the multi-year ice region north of the CAA into the Beaufort Sea as in Long-CTRL. This suggests that the overestimation is not mainly due to biases in the atmospheric forcing but imperfect model parameterizations and initial ice-ocean conditions.

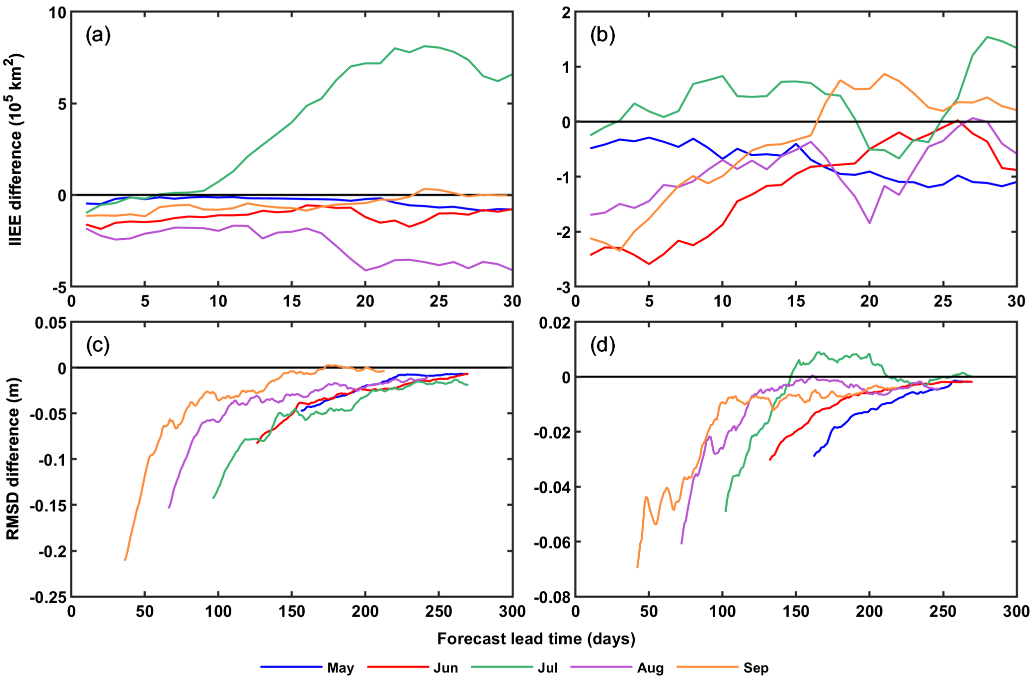

Figure 3. The difference of the IIEE ($10^5 km^2$) in 2015 (a) and in 2016 (b), and the difference of the RMSD of the SIT (m) in 2015 (c) and in 2016 (d) between the Long-SIT and Long-CTRL forecasts initialized from May to September. The RMSD of the SIT is computed with respect to the CS2SMOS product available from October to April, hence the staggered time series in (c) and (d). Note that negative values indicate better forecast skill.

4 Summary

This study examines the impact of summer CryoSat-2 SIT assimilation on short- and long-term sea-ice forecasts in 2015 and in 2016. The ice-edge forecasts with summer CryoSat-2 SIT assimilation are dramatically improved when compared to the experiments without any data assimilation. When the summer CryoSat-2 SIT data are assimilated together with SIC data, the effects on the ice-edge forecast skill are rather dependent on the time when the forecast is initialized and are spatially highly variable. In the Pacific sector, the combined assimilation of summer SIT and SIC observations leads to more realistic summer ice-edge forecasts with a one-week lead time.

The long-term sea-ice forecasts show significant reductions in both IIEE and RMSD of the SIT, except for those initialized in July, when the summer CryoSat-2 SIT has large uncertainties. The improvement in ice-edge forecasts can last up to about 30 days, while for the SIT forecasts the benefits can last for more than 3 months. This result demonstrates that, although the atmospheric forecasts used to drive the model can evolve freely after about one month, the SIT initialization in summer remains a primary factor in predicting long-term SIT variations.

However, limitations of the summer CryoSat-2 SIT data product still remain. The deep learning algorithm used has a certain degree of uncertainty in classifying ice leads and melt ponds, especially when the melt-pond fraction is large. The underestimation in the summer CryoSat-2 SIT from July to September in the coastal regions north of the CAA and Greenland requires further work on the sea-ice freeboard and thickness retrieval algorithm or exploration of new correction schemes to improve their reliability and accuracy. Furthermore, it is still an open question how this product should be used for real-time Arctic sea-ice forecasting, since its uncertainty currently does not account for all the algorithm errors, and possible representation errors (Janjić et al., 2018) should be considered accurately.

5 Open Research

The ensemble mean Arctic sea-ice thickness (SIT) and sea-ice concentration (SIC) forecast data used in the study can be downloaded at Song et al. (2024). The file size of the forecast results with all ensemble members exceeds 50GB and can be made available upon request through contact. The CMST SIT estimate is available at Mu et al. (2018a). The summer CryoSat-2 SIT observations can be downloaded from Landy and Dawson (2022). The SSMI/SSMIS SIC data is avaliable from Kern et al. (2024). The UKMO atmospheric ensemble forecasts are avaliable in the THORPEX Interactive Grand Global Ensemble (TIGGE; Bougeault et al., 2010) archive (`https://apps.ecmwf.int/datasets/data/tigge`). The hourly ERA5 reanalysis is avaliable at Hersbach et al. (2023). The CFSv2 atmospheric forecasts are avaliable at `https://www.ncei.noaa.gov/products/weather-climate-models/climate-forecast-system`. The PIOMAS (J. Zhang & Rothrock, 2003) data is provided at `https://psc.apl.uw.edu/data`. The NOAA/NSIDC SIC CDR data is avaliable at Meier et al. (2021). The CS2SMOS data is avaliable at `https://www.meereisportal.de`. Mooring observations from BGEP are downloaded from `https://www2.whoi.edu/site/beaufortgyre`.

Acknowledgments

This study is supported by the National Key R&D Program of China under Grant 2019YFA0607000, the National Natural Science Foundation of China (42176235) and the Laoshan Laboratory (LSKJ202202300). Contribution of SNL was supported by the Federal Ministry of Education and Research of Germany in the framework of the Seamless Sea Ice Prediction project (SSIP, Grant 01LN1701A) and partly made in the framework of the state assignment of SIO RAS (theme FMWE-2024-0028).

References

Blanchard-Wrigglesworth, E., Bitz, C. M., & Holland, M. M. (2011, 09). Influence of initial conditions and climate forcing on predicting arctic sea ice. *Geophysical Research Letters*, *38*, L18503. doi: 10.1029/2011GL048807

Blockley, E. W., & Peterson, K. A. (2018). Improving met office seasonal predictions of arctic sea ice using assimilation of cryosat-2 thickness. *The Cryosphere*, *12*(11), 3419-3438. doi: 10.5194/tc-12-3419-2018

Bougeault, P., Toth, Z., Bishop, C., Brown, B., Burridge, D., Chen, D. H., … Worley, S. (2010). The thorpex interactive grand global ensemble. *Bulletin of the American Meteorological Society*, *91*(8), 1059-1072. doi: 10.1175/2010BAMS2853.1

Bowler, N. E., Arribas, A., Mylne, K. R., Robertson, K. B., & Beare, S. E. (2008). The mogreps short–range ensemble prediction system. *Quarterly Journal of the Royal Meteorological Society*, *134*(632), 703–722. doi: 10.1002/qj.234

Bushuk, M., Msadek, R., Winton, M., Vecchi, G. A., Gudgel, R., Rosati, A., & Yang, X. (2017). Skillful regional prediction of arctic sea ice on seasonal timescales. *Geophysical Research Letters*, *44*(10), 4953-4964. doi: 10.1002/2017GL073155

Bushuk, M., Winton, M., Bonan, D. B., Blanchard-Wrigglesworth, E., & Delworth, T. L. (2020). A mechanism for the arctic sea ice spring predictability barrier. *Geophysical Research Letters*, *47*(13), e2020GL088335. doi: 10.1029/2020GL088335

Bushuk, M., Zhang, Y., Winton, M., Hurlin, B., Delworth, T., Lu, F., … Zeng, F. (2022, 07). Mechanisms of regional arctic sea ice predictability in two dynamical seasonal forecast systems. *Journal of Climate*, *35*, 4207-4231. doi: 10.1175/JCLI-D-21-0544.1

Comiso, J. C., Parkinson, C. L., Gersten, R., & Stock, L. (2008). Accelerated decline in the arctic sea ice cover. *Geophysical Research Letters*, *35*(1), L01703. doi: 10.1029/2007GL031972

Dawson, G., Landy, J., Tsamados, D. M., Komarov, A. S., Howell, S., Heorton, H., & Krumpen, T. (2022, 01). A 10-year record of arctic summer sea ice freeboard from cryosat-2. *Remote Sensing of Environment*, *268*, 112744. doi: 10.1016/j.rse.2021.112744

Day, J. J., Hawkins, E., & Tietsche, S. (2014). Will arctic sea ice thickness initialization improve seasonal forecast skill? *Geophysical Research Letters*, *41*, 7566-7575. doi: 10.1002/2014GL061694

Day, J. J., Tietsche, S., & Hawkins, E. (2014). Pan-arctic and regional sea ice predictability: initialization month dependence. *Journal of Climate*, *27*(12), 4371-4390. doi: 10.1175/JCLI-D-13-00614.1

Dirkson, A., Merryfield, W. J., & Monahan, A. H. (2017). Impacts of sea ice thickness initialization on seasonal arctic sea ice predictions. *Journal of Climate*, *30*, 1001-1017. doi: 10.1175/JCLI-D-16-0437.1

Drinkwater, M. R. (1991). K $_u$ band airborne radar altimeter observations of marginal sea ice during the 1984 marginal ice zone experiment. *Journal of Geophysical Research: Oceans*, *96*(C3), 4555-4572. doi: 10.1029/90JC01954

Feng, J., Zhang, Y., Cheng, Q., & Tsou, J. Y. (2022). Pan-arctic melt pond fraction trend, variability, and contribution to sea ice changes. *Global and Planetary Change*, *217*, 103932. doi: 10.1016/j.gloplacha.2022.103932

Goessling, H. F., Tietsche, S., Day, J. J., Hawkins, E., & Jung, T. (2016). Predictability of the arctic sea-ice edge. *Geophysical Research Letters*, *43*, 1642–1650. doi: 10.1002/2015GL067232

Guemas, V., Blanchard-Wrigglesworth, E., Chevallier, M., Day, J. J., Déqué, M., Doblas-Reyes, F. J., … Tietsche, S. (2016). A review on arctic sea ice predictability and prediction on seasonal-to-decadal timescales. *Quarterly Journal of the Royal Meteorological Society*, *142*, 546-561. doi: 10.1002/qj.2401

Hebert, D. A., Allard, R. A., Metzger, E. J., Posey, P. G., Preller, R. H., Wallcraft, A. J., … Smedstad, O. M. (2015, 11). Short-term sea ice forecasting: An assessment of ice concentration and ice drift forecasts using the u.s. navy's arctic cap nowcast/forecast system. *Journal of Geophysical Research: Oceans*, *120*, 8327-8345. doi: 10.1002/2015JC011283

Hersbach, H., Bell, B., Berrisford, P., Biavati, G., Horányi, A., Muñoz Sabater, J., … Thépaut, J.-N. (2023). *Era5 hourly data on single levels from 1940 to present* [dataset]. Copernicus Climate Change Service (C3S) Climate Data Store (CDS). Retrieved from `https://cds.climate.copernicus.eu/cdsapp#!/dataset/reanalysis-era5-single-levels?tab=overview` doi: 10.24381/cds.adbb2d47

Hersbach, H., Bell, B., Berrisford, P., Hirahara, S., Horányi, A., Muñoz-Sabater, J., … Thépaut, J.-N. (2020). The era5 global reanalysis. *Quarterly Journal of the Royal Meteorological Society*, 1999–2049. doi: 10.1002/qj.3803

Hibler III, W. D. (1979). A dynamic thermodynamic sea ice model. *Journal of Physical Oceanography*, *9*, 815-846. doi: 10.1175/1520-0485(1979)009<0815:ADTSIM>2.0.CO;2

Janjić, T., Bormann, N., Bocquet, M., Carton, J. A., Cohn, S. E., Dance, S. L., … Weston, P. (2018). On the representation error in data assimilation. *Quarterly Journal of the Royal Meteorological Society*, *144*(713), 1257-1278. doi: 10.1002/qj.3130

Jung, T., Gordon, N. D., Bauer, P., Bromwich, D. H., Chevallier, M., Day, J. J., … Yang, Q. (2016). Advancing polar prediction capabilities on daily to seasonal time scales. *Bulletin of the American Meteorological Society*, *97*, 160113112747009. doi: 10.1175/BAMS-D-14-00246.1

Kaleschke, L., Lüpkes, C., Vilna, T., Haarpaintner, J., Borchert, A., Hartmann, J., & Heygster, G. (2001). Ssm/i sea ice remote sensing for mesoscale ocean-atmosphere interaction analysis. *Canadian Journal of Remote Sensing*, *27*, 526-537. doi: 10.1080/

07038992.2001.10854892

Kern, S., Kaleschke, L., Girard-Ardhuin, F., Spreen, G., & Beitsch, A. (2024). *Global daily gridded 5-day median-filtered, gap-filled asi algorithm ssmi-ssmis sea ice concentration data* [dataset]. Integrated Climate Date Center. Retrieved from `https://www.cen.uni-hamburg.de/en/icdc/data/cryosphere/seaiceconcentration-asi-ssmi.html`

Kern, S., Kaleschke, L., & Spreen, G. (2010). Climatology of the nordic (irminger, greenland, barents, kara and white/pechora) seas ice cover based on 85 ghz satellite microwave radiometry: 1992–2008. *Tellus A*, *62*, 411-434. doi: 10.3402/tellusa.v62i4.15709

Kwok, R., & Rothrock, D. A. (2009). Decline in arctic sea ice thickness from submarine and icesat records: 1958-2008. *Geophysical Research Letters*, *36*, L15501. doi: 10.1029/2009GL039035

Landrum, L., & Holland, M. M. (2020, 12). Extremes become routine in an emerging new arctic. *Nature Climate Change*, *10*, 1-8. doi: 10.1038/s41558-020-0892-z

Landy, J. C., & Dawson, G. J. (2022). *Year-round arctic sea ice thickness from cryosat-2 baseline-d level 1b observations 2010-2020 (version 1.0)* [dataset]. NERC EDS UK Polar Data Centre. Retrieved from `https://data.bas.ac.uk/full-record.php?id=GB/NERC/BAS/PDC/01613` doi: 10.5285/d8c66670-57ad-44fc-8fef-942a46734ecb

Landy, J. C., Dawson, G. J., Tsamados, M., Bushuk, M., Stroeve, J. C., Howell, S. E. L., … Aksenov, Y. (2022). A year-round satellite sea-ice thickness record from cryosat-2. *Nature*, *609*, 1-6. doi: 10.1038/s41586-022-05058-5

Laxon, S. W., Giles, K. A., Ridout, A. L., Wingham, D. J., Willatt, R., Cullen, R., … Davidson, M. (2013). Cryosat-2 estimates of arctic sea ice thickness and volume. *Geophysical Research Letters*, *40*(4), 732-737. doi: 10.1002/grl.50193

Lee, S., Kim, H.-C., & Im, J. (2018). Arctic lead detection using a waveform mixture algorithm from cryosat-2 data. *The Cryosphere*, *12*(5), 1665-1679. doi: 10.5194/tc-12-1665-2018

Lemieux, J.-F., Beaudoin, C., Dupont, F., Roy, F., Smith, G. C., Shlyaeva, A., … Ferry, N. (2015, 03). The regional ice prediction system (rips): Verification of forecast sea ice concentration. *Quarterly Journal of the Royal Meteorological Society*, *142*, 632-643. doi: 10.1002/qj.2526

Losch, M., Menemenlis, D., Campin, J.-M., Heimbach, P., & Hill, C. (2010). On the formulation of sea-ice models. part 1: Effects of different solver implementations and parameterizations. *Ocean Modelling*, *33*(1), 129-144. doi: 10.1016/j.ocemod.2009.12.008

Marshall, J., Adcroft, A., Hill, C., Perelman, L., & Heisey, C. (1997). A finite-volume, incompressible navier stokes model for studies of the ocean on parallel computers. *Journal of Geophysical Research*, *102*, 5753-5766. doi: 10.1029/96JC02775

Maykut, G. A., Grenfell, T. C., & Weeks, W. (1992). On estimating spatial and temporal variations in the properties of ice in the polar oceans. *Journal of Marine Systems*, *3*, 41-72. doi: 10.1016/0924-7963(92)90030-C

Meier, W. N., Fetterer, F., Windnagel, A. K., & Stewart., J. S. (2021). *Noaa/nsidc climate data record of passive microwave sea ice concentration, version 4* [dataset]. National Snow and Ice Data Center. Retrieved from `https://nsidc.org/data/G02202/versions/4` doi: 10.7265/efmz-2t65

Mignac, D., Martin, M., Fiedler, E., Blockley, E., & Fournier, N. (2022, 02). Improving the met office's forecast ocean assimilation model (foam) with the assimilation of satellite-derived sea-ice thickness data from cryosat-2 and smos in the arctic. *Quarterly Journal of the Royal Meteorological Society*, *148*, 1-24. doi: 10.1002/qj.4252

Min, C., Yang, Q., Luo, H., Chen, D., Krumpen, T., Mamnun, N., … Nerger, L. (2023). Improving arctic sea-ice thickness estimates with the assimilation of cryosat-2 summer observations. *Ocean-Land-Atmosphere Research*, *2*, 0025. doi: 10.34133/olar.0025

Mu, L., Liang, X., Yang, Q., Liu, J., & Zheng, F. (2019). Arctic ice ocean prediction system: evaluating sea ice forecasts during xuelong's first trans-arctic passage in summer 2017. *Journal of Glaciology*, 1-9. doi: 10.1017/jog.2019.55

Mu, L., Losch, M., Yang, Q., Ricker, R., Losa, S. N., & Nerger, L. (2018a). *The arc-*

tic combined model and satellite sea ice thickness (cmst) dataset [dataset]. PANGAEA. Retrieved from https://doi.org/10.1594/PANGAEA.891475 doi: 10.1594/PANGAEA.891475

Mu, L., Losch, M., Yang, Q., Ricker, R., Losa, S. N., & Nerger, L. (2018b). Arctic-wide sea ice thickness estimates from combining satellite remote sensing data and a dynamic ice-ocean model with data assimilation during the cryosat-2 period. *Journal of Geophysical Research: Oceans*, *123*, 7763-7780. doi: 10.1029/2018JC014316

Mu, L., Nerger, L., Streffing, J., Tang, Q., Niraula, B., Zampieri, L., … Goessling, H. F. (2022). Sea-ice forecasts with an upgraded awi coupled prediction system. *Journal of Advances in Modeling Earth Systems*, *14*(12), e2022MS003176. doi: 10.1029/2022MS003176

Mu, L., Yang, Q., Losch, M., Losa, S. N., Ricker, R., Nerger, L., & Liang, X. (2017). Improving sea ice thickness estimates by assimilating cryosat-2 and smos sea ice thickness data simultaneously: Cryosat-2 and smos sea ice thickness data assimilation. *Quarterly Journal of the Royal Meteorological Society*, *144*, 529-538. doi: 10.1002/qj.3225

Nerger, L., Hibler III, W. D., & SCHRÖTER, J. (2005). Pdaf-the parallel data assimilation framework: Experiences with kalman filtering. *World Scientific*, 63–83. doi: 10.1142/9789812701831_0006

Nerger, L., Janjić, T., Schröter, J., & Hiller, W. (2012). A regulated localization scheme for ensemble-based kalman filters. *Quarterly Journal of the Royal Meteorological Society*, *138*(664), 802-812. doi: 10.1002/qj.945

Nguyen, A. T., Menemenlis, D., & Kwok, R. (2011). Arctic ice-ocean simulation with optimized model parameters: Approach and assessment. *Journal of Geophysical Research: Oceans*, *116*, C04025. doi: 10.1029/2010JC006573

Parkinson, C. L., & Washington, W. M. (1979). A large-scale numerical model of sea ice. *Journal of Geophysical Research*, *84*, 311-337. doi: 10.1029/JC084iC01p00311

Posey, P., Metzger, E., Wallcraft, A., Hebert, D., Allard, R., Smedstad, O., … Helfrich, S. (2015, 08). Improving arctic sea ice edge forecasts by assimilating high horizontal resolution sea ice concentration data into the us navy's ice forecast systems. *The Cryosphere*, *9*, 1735-1745. doi: 10.5194/tc-9-1735-2015

Ricker, R., Hendricks, S., Helm, V., Skourup, H., & Davidson, M. (2014). Sensitivity of cryosat-2 arctic sea-ice freeboard and thickness on radar-waveform interpretation. *The Cryosphere*, *8*, 1607-1622. doi: 10.5194/tc-8-1607-2014

Ricker, R., Hendricks, S., Kaleschke, L., Tian-Kunze, X., King, J., & Haas, C. (2017). A weekly arctic sea-ice thickness data record from merged cryosat-2 and smos satellite data. *The Cryosphere*, *11*(4), 1607–1623. doi: 10.5194/tc-11-1607-2017

Rothrock, D. A., Yu, Y., & Maykut, G. A. (1999). Thinning of the arctic sea-ice cover. *Geophysical Research Letters*, *26*, 3469-3472. doi: 10.1029/1999GL010863

Saha, S., Moorthi, S., Wu, X., Wang, J., Nadiga, S., Tripp, P., … Becker, E. (2014). The ncep climate forecast system version 2. *Journal of Climate*, *27*, 2185–2208. doi: 10.1175/JCLI-D-12-00823.1

Schlitzer, R. (2023). *Ocean data view* [software]. Retrieved from https://odv.awi.de

Semtner, A. J. (1976). A model for thermodynamic growth of sea ice in numerical investigations if climate. *Journal of Physical Oceanography*, *6*, 379-389. doi: 10.1175/1520-0485(1976)006<0379:AMFTTG>2.0.CO;2

Shu, Q., Qiao, F., Liu, J., Song, Z., Chen, Z., Zhao, J., … Song, Y. (2021). Arctic sea ice concentration and thickness data assimilation in the fio-esm climate forecast system. *Acta Oceanologica Sinica*, *40*, 65-75. doi: 10.1007/s13131-021-1768-4

Song, R., Mu, L., Kauker, F., Loza, S., & Chen, X. (2024). *Forecast data for the paper: "assimilating summer sea-ice thickness observations improves arctic sea-ice forecast"* [dataset]. Zenodo. Retrieved from https://doi.org/10.5281/zenodo.10589315 doi: 10.5281/zenodo.10589315

Spreen, G., Kaleschke, L., & Heygster, G. (2008). Sea ice remote sensing using amsr-e 89-ghz channels. *Journal of Geophysical Research*, *113*, C02S03. doi: 10.1029/2005JC003384

Stroeve, J. C., Serreze, M. C., Holland, M. M., Kay, J. E., Malanik, J., & Barrett, A. P.

(2012, 02). The arctic's rapidly shrinking sea ice cover: A research synthesis. *Climatic Change*, *110*, 1005-1027. doi: 10.1007/s10584-011-0101-1

Tilling, R., Ridout, A., & Shepherd, A. (2019). Assessing the impact of lead and floe sampling on arctic sea ice thickness estimates from envisat and cryosat-2. *Journal of Geophysical Research: Oceans*, *124*, 7473–7485. doi: 10.1029/2019JC015232

Xie, J., Counillon, F., Bertino, L., Tian-Kunze, X., & Kaleschke, L. (2016). Benefits of assimilating thin sea ice thickness from smos into the topaz system. *The Cryosphere*, *10*, 2745–2761. doi: 10.5194/tc-10-2745-2016

Xiong, C., & Ren, Y. (2023). Arctic sea ice melt pond fraction in 2000–2021 derived by dynamic pixel spectral unmixing of modis images. *ISPRS Journal of Photogrammetry and Remote Sensing*, *197*, 181-198. doi: 10.1016/j.isprsjprs.2023.01.023

Yang, Q., Losa, S. N., Losch, M., Jung, T., & Nerger, L. (2015). The role of atmospheric uncertainty in arctic summer sea ice data assimilation and prediction. *Quarterly Journal of the Royal Meteorological Society*, *141*, 2314-2323. doi: 10.1002/qj.2523

Yang, Q., Losa, S. N., Losch, M., Liu, J., Zhang, Z., Nerger, L., & Yang, H. (2015). Assimilating summer sea-ice concentration into a coupled ice–ocean model using a lseik filter. *Annals of Glaciology*, *56*(69), 38–44. doi: 10.3189/2015AoG69A740

Yang, Q., Losch, M., Losa, S. N., Jung, T., Nerger, L., & Lavergne, T. (2016). Brief communication: The challenge and benefit of using sea ice concentration satellite data products with uncertainty estimates in summer sea ice data assimilation. *The Cryosphere*, *10*, 761-774. doi: 10.5194/tc-10-761-2016

Zhang, J., & Hibler III, W. D. (1997). On an efficient numerical method for modeling sea ice dynamics. *Journal of Geophysical Research*, *102*, 8691–8702. doi: 10.1029/96JC03744

Zhang, J., & Rothrock, D. A. (2003). Modeling global sea ice with a thickness and enthalpy distribution model in generalized curvilinear coordinates. *Monthly Weather Review*, *131*, 845–861. doi: 10.1175/1520-0493(2003)131<0845:MGSIWA>2.0.CO;2

Zhang, Y.-F., Bushuk, M., Winton, M., Hurlin, B., Gregory, W., Landy, J., & Jia, L. (2023). Improvements in september arctic sea ice predictions via assimilation of summer cryosat-2 sea ice thickness observations. *Geophysical Research Letters*, *50*(24), e2023GL105672. doi: 10.1029/2023GL105672

Supporting Information for "Assimilating summer sea-ice thickness observations improves Arctic sea-ice forecast"

Ruizhe Song[1,2,3,4], Longjiang Mu[2], Svetlana N. Loza[3,5], Frank Kauker[3],

Xianyao Chen[1,2]

[1]Frontier Science Center for Deep Ocean Multispheres and Earth System and Physical Oceanography Laboratory, Ocean University of China, Qingdao, China

[2]Laoshan Laboratory, Qingdao, China

[3]Alfred Wegener Institute, Helmholtz Centre for Polar and Marine Research, Bremerhaven, Germany

[4]Academy of the Future Ocean, Ocean University of China, Qingdao, China

[5]Shirshov Institute of Oceanology, Russian Academy of Sciences, Moscow, Russia

Contents of this file

Uncertainty of CryoSat-2 summer SIT observation used in the assimilation and forecast system

---

Corresponding author: Longjiang Mu, ljmu@qnlm.ac

The observation uncertainty used in the assimilation and forecast system includes measurement errors and representation errors (Janjić et al., 2018). Considering the underestimation of the CryoSat-2 (CS2) summer SIT observations, in our study, the total uncertainty (σ) is determined by taking into account both the observational errors (σ_{CS2}) provided in the CS2 SIT dataset and the corrected errors (σ_{corr}) estimated based on the spatial distribution of the CMST SIT, as $\sigma = max(\sigma_{CS2}, \sigma_{corr})$. We take a piecewise form for σ_{corr}, which is a function of the SIT of a reference product. It is set to 0.5 m when CMST SIT values are between 2.5 and 3.0 m, and 1.0 m when CMST SIT is greater than 4.0 m. A linear interpolation between 0.5 and 1.0 m is utilized for the CMST SIT between 3.0-4.0 m. Note that this correction is most important when the CS2 SIT uncertainty peaks annually, specifically in the range of 0.4-0.8 m in multi-year ice regions from July to August.

References

Janjić, T., Bormann, N., Bocquet, M., Carton, J. A., Cohn, S. E., Dance, S. L., ... Weston, P. (2018). On the representation error in data assimilation. *Quarterly Journal of the Royal Meteorological Society*, *144*(713), 1257-1278. doi: 10.1002/qj.3130

Schlitzer, R. (2023). *Ocean data view* [software]. Retrieved from `https://odv.awi.de`

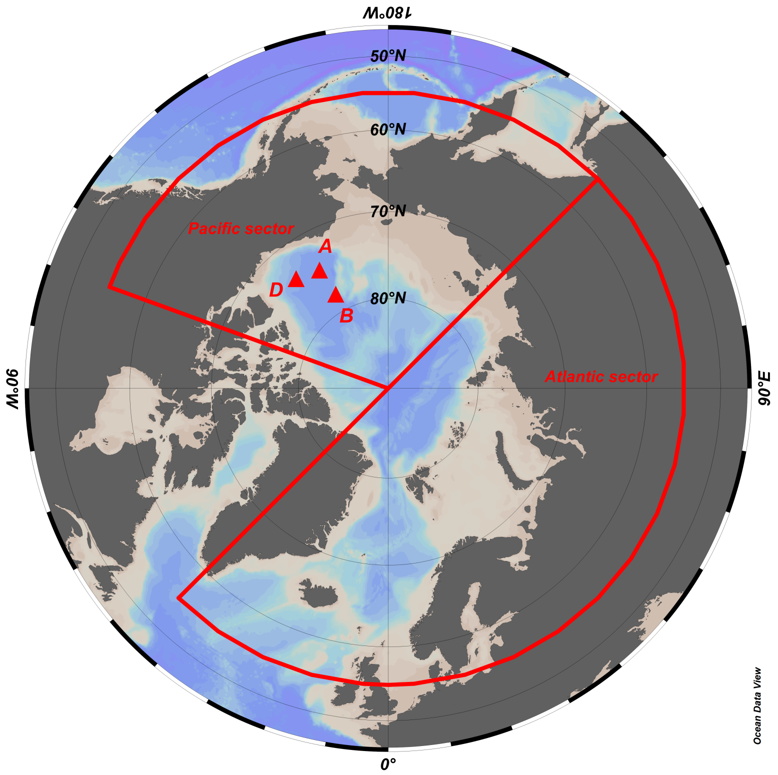

Figure S1. Study area of ice-edge forecasts and the location of BGEP moorings. This figure is plotted with Ocean Data View (Schlitzer, 2023).

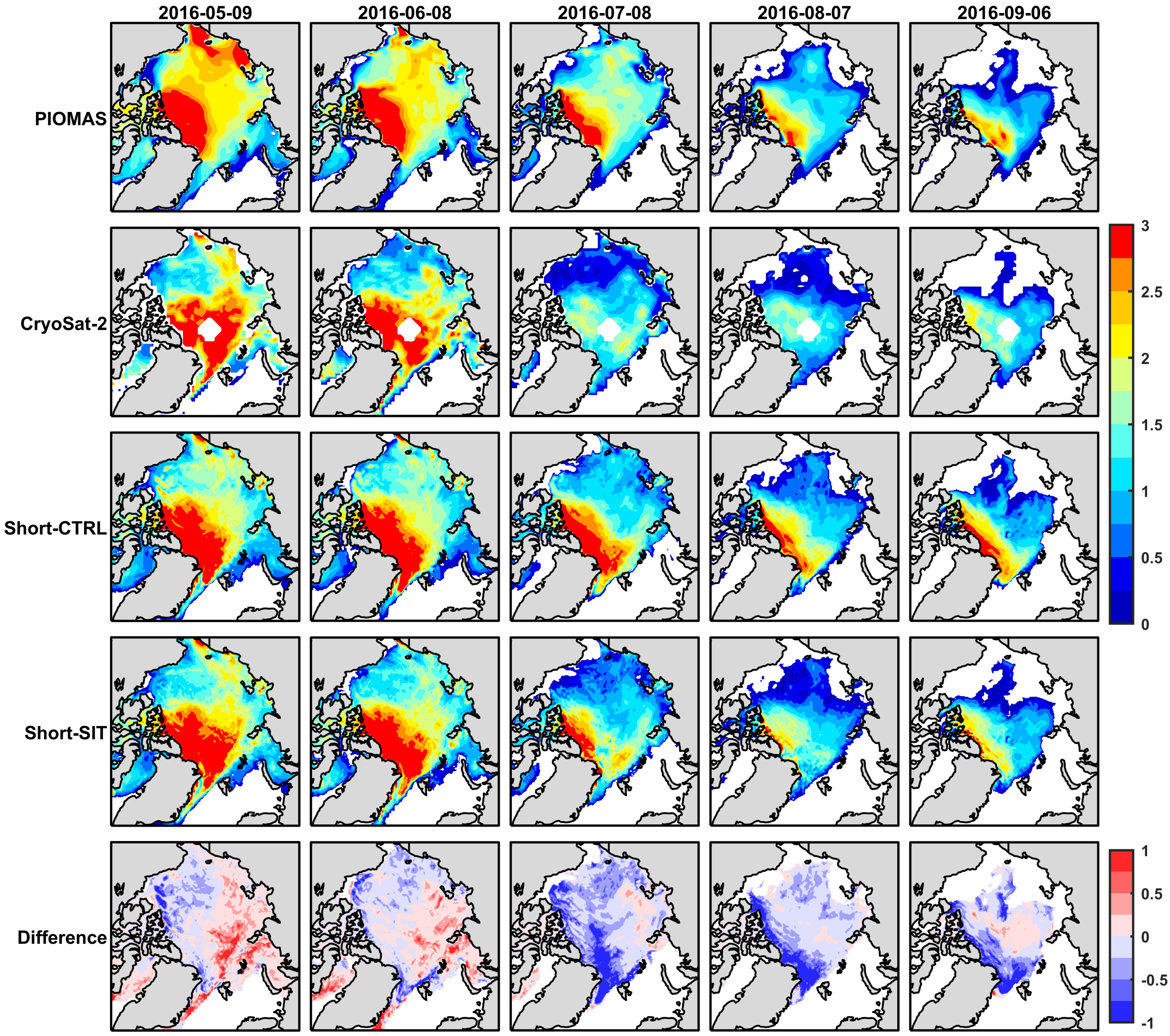

Figure S2. Same as Figure 1, but in 2016

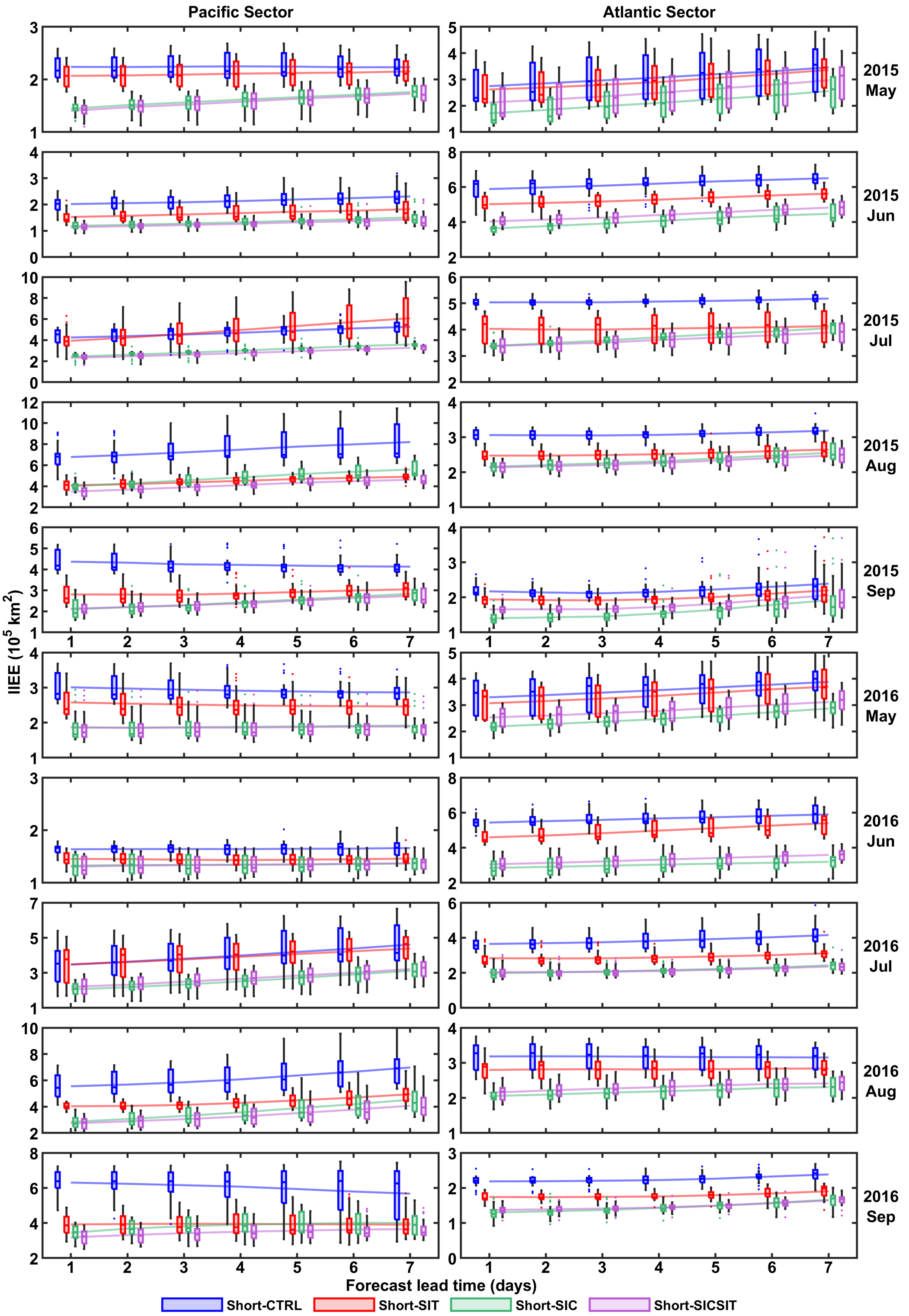

Figure S3. Box plot of IIEE. The forecasted IIEE is calculated after 7 days of assimilation, when the summer CryoSat-2 SIT takes full effect. Blue, red, green, and purple boxes refer to IIEE in Short-CTRL, Short-SIT, Short-SIC, and Short-SICSIT, respectively. Colored boxes indicate IIEE between the lower and upper quartiles. Colored outliers denote values more than 1.5 interquartile range away from the top or bottom of the box. The outer edges of the black lines denote the minimum and maximum of the values that are not outliers. Solid lines show the mean IIEE in each month and region.

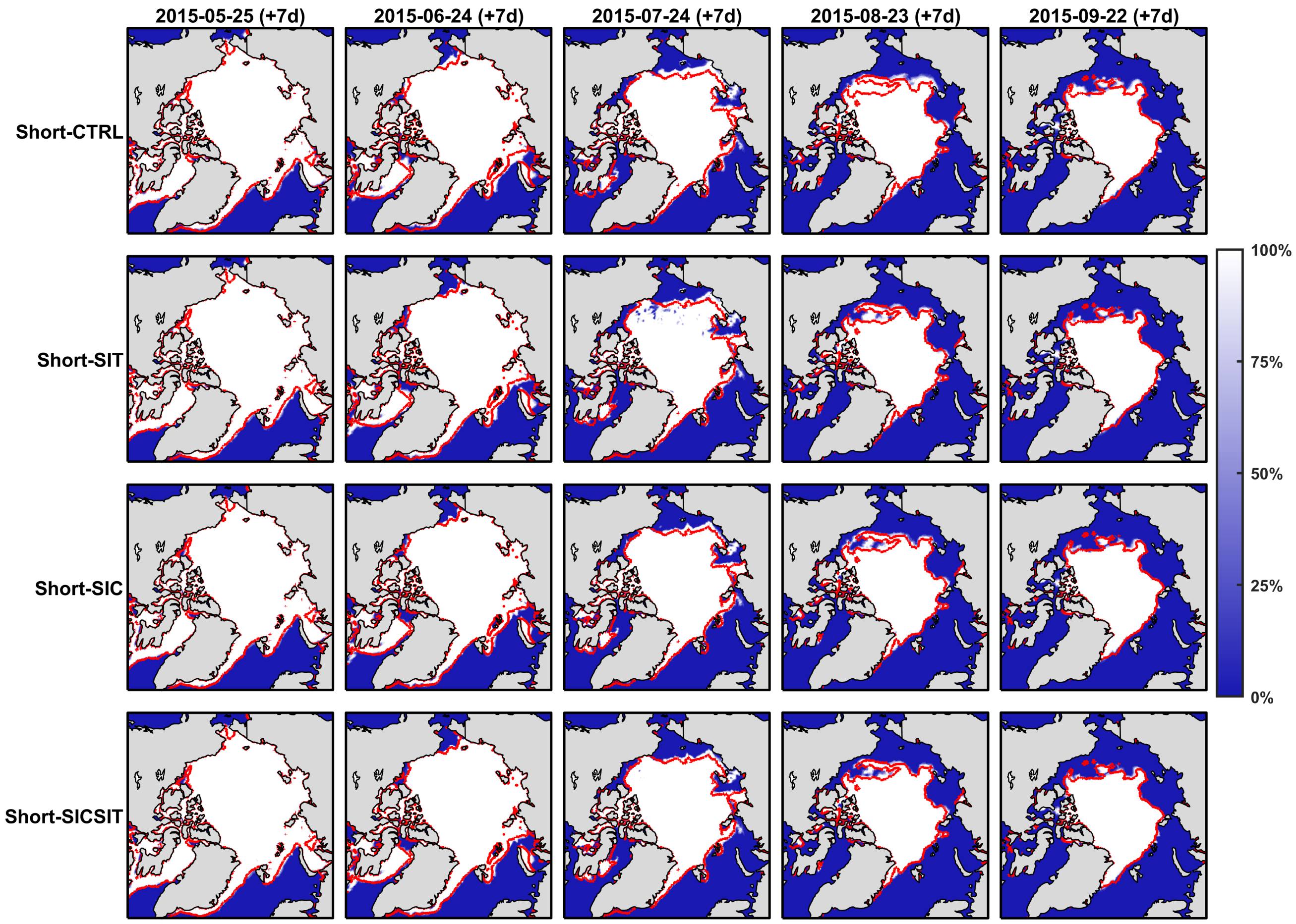

Figure S4. The 7-day lead time ice-edge forecasts from the 18th day after the initialization in May to September in 2015. Red lines indicate the NSIDC observed ice edge. The color scale shows the sea-ice probability computed from the 11 ensemble members.

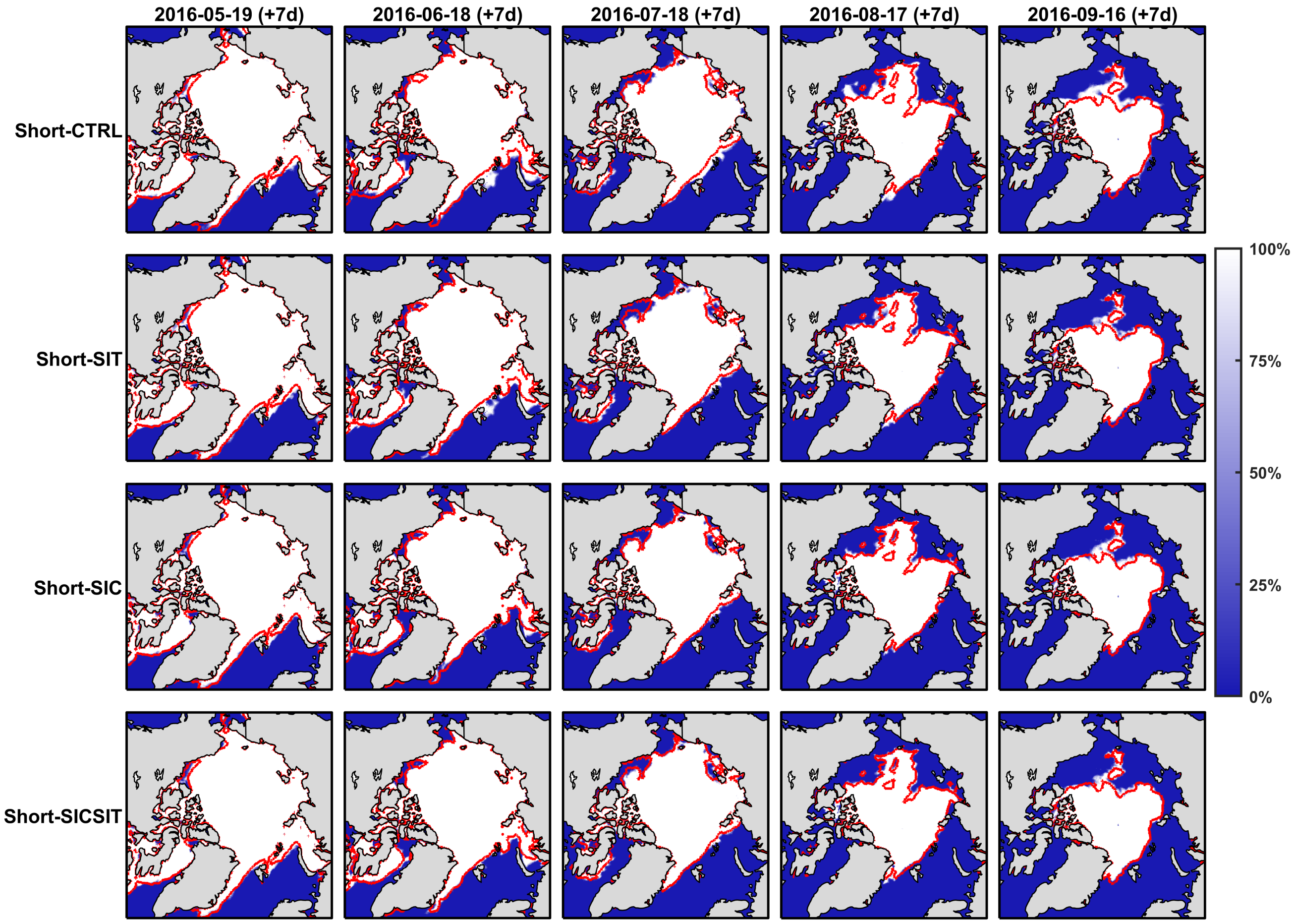

Figure S5. Same as Figure S4, but in 2016

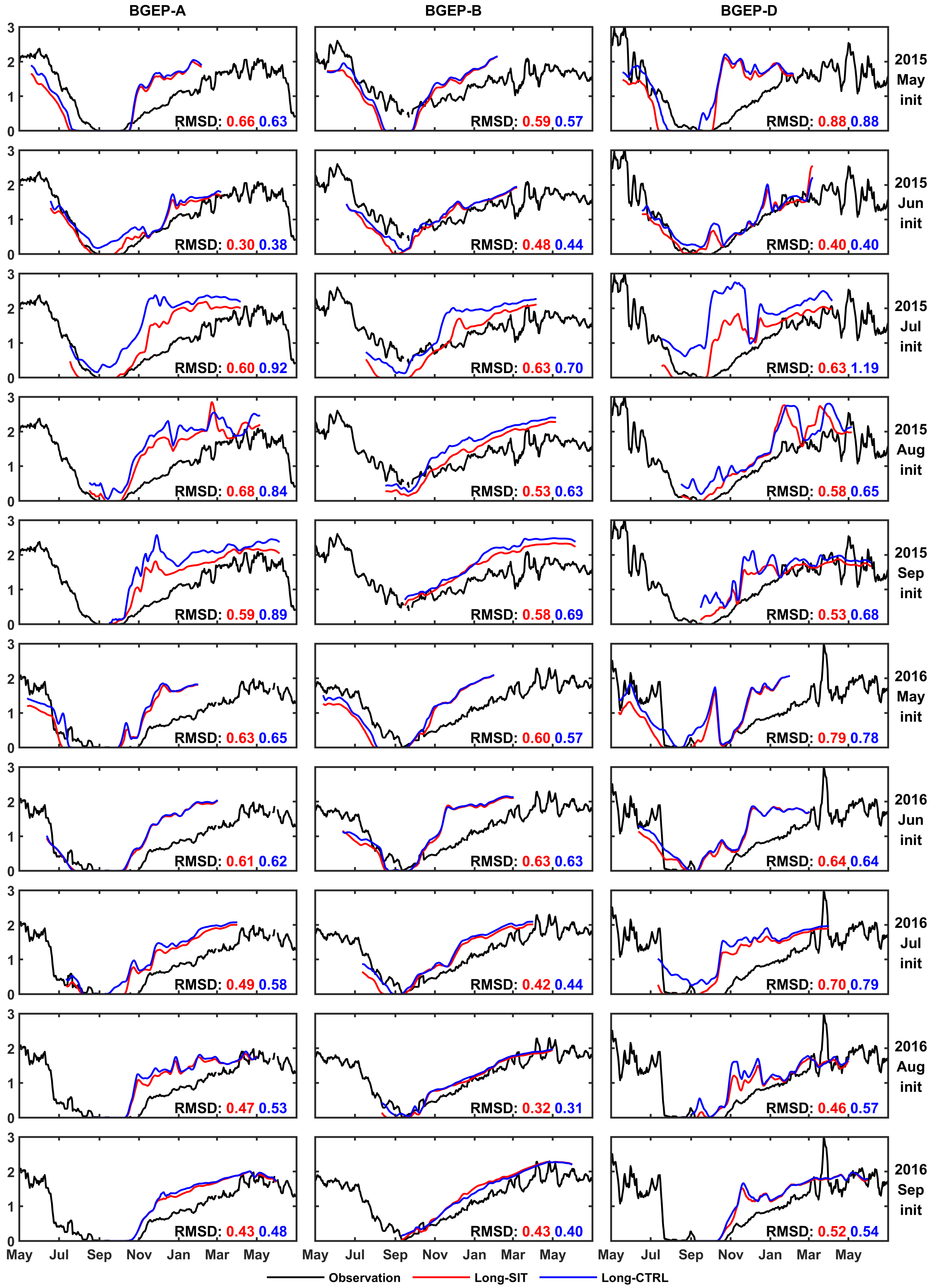

January 31, 2024, 5:30pm

Figure S6. Long-term SIT forecasts at the sites of BGEP-A, BGEP-B, and BGEP-D. Black lines show the 7-day average SIT from the BGEP ULS, red lines indicate the SIT from Long-SIT, while blue lines show the SIT from Long-CTRL.